SPE 107705

Production Data Analysis of CBM Wells

C.R. Clarkson, SPE, ConocoPhillips Canada; C.L. Jordan, SPE, Apache Canada Ltd.; R. R. Gierhart, SPE, BP; and J.P. Seidle, SPE, MHA Petroleum Consultants

This paper was prepared for presentation at the 2007 SPE Rocky Mountain Oil & Gas Technology Symposium held in Denver, Colorado, U.S.A., 16–18 April 2007.

Abstract

Recent advances in production data analysis (PDA) techniques have greatly assisted engineers in extracting meaningful reservoir and stimulation information from well production and flowing pressure data. Application of these techniques to coalbed methane (CBM) reservoirs requires that the unique coal storage and transport properties be accounted for. In recent work, the authors and others have demonstrated how new techniques such as the flowing material balance (FMB) and production type-curves may be adapted to account for CBM storage mechanisms (i.e. adsorption), but to date the focus has been on relatively simple CBM reservoir behavior. Although adaptations of PDA to include more complex CBM reservoir characteristics were introduced, the focus of the current work is advancement of modern PDA techniques to incorporate reservoir behavior such as single-phase flow of water in undersaturated reservoirs, two-phase (gas+water) flow in saturated reservoirs, effective permeability changes during depletion, and changing gas composition due to relative adsorption. Specifically, the FMB technique is modified in this work to include several complex CBM reservoir characteristics. FMB can be a powerful diagnostic technique when relative and absolute permeability changes are apparent during depletion. Several synthetic and field examples are given to demonstrate how FMB, type-curve analysis and analytical simulation can be used in parallel to provide a particularly useful data analysis tool.

The adapted PDA techniques used in this work make use of the pseudotime and pseudopressure concepts, modified to account for CBM reservoir behavior, to linearize the (constant-rate) diffusivity equation for CBM. Material balance pseudotime was used to account for variable operating conditions. These techniques were used successfully to extract quantitative reservoir information from single- and two-phase CBM simulated and field production and pressure data. The techniques for two-phase CBM require further evaluation, however.

Several key assumptions were used in deriving the PDA techniques including (but not limited to) instantaneous desorption (small sorption times) and single-layer behavior. Although the former is not considered a serious limitation, as most commercial reservoirs analyzed to date by the authors have exhibited single-porosity behavior during production, the latter may be quite important for some producing fields. PDA of multi-layered CBM reservoirs will be discussed at length in a future paper.

Introduction

Over the past several decades, significant advances have been made in production data analysis (PDA) of conventional oil and gas reservoirs[1-10] (select references given only). Although numerical reservoir simulation certainly qualifies as a PDA technique, we limit our discussion mainly to FMB, and production type-curves, used, in some instances, in parallel with analytical simulation. These modern methods have greatly enhanced the engineers' ability to obtain quantitative information about reservoir properties and stimulation/damage from data that is routinely gathered during the producing life of a well, such as production data, and in some instances, flowing pressure information. The information that may be obtained from detailed production data analysis includes oil or gas-in-place (GIP), permeability-thickness product (kh) and skin (s), and can be used to supplement information obtained from other sources such as pressure transient analysis (PTA), material balance and reservoir simulation.

Complex reservoir behavior encountered in CBM plays has precluded analysis using modern PDA techniques, such as FMB, until recently. The analyst could be faced with several reservoir complexities during primary depletion of a CBM reservoir, depending upon the CBM play of interest, such as:

- Gas storage by adsorption and free-gas compression in the pore space.
- Relative permeability effects in two-phase (gas+water) coals.
- Stress- and/or desorption-dependent fracture pore volume and absolute permeability.
- Multi-layer characteristics caused by contrasting permeability from coal seam to seam, that have limited or no vertical communication.
- Dual porosity behavior, when sorption times are large.

- Permeability anisotropy caused by contrasting permeabilities in the direction of each natural fracture set.
- Lateral changes in reservoir properties.
- Changing composition of produced free-gas due to relative adsorption effects and or diffusion times of the gas components.

Previous work discussing application of modern PDA methods, such as type-curve and flowing material balance (FMB), has focused mainly on relatively simple CBM reservoir behavior. Pinzon and Patterson[11] applied a modified Fetkovich type-curve, using pseudotime accounting for gas desorption (as described in Spivey and Semmelbeck[12]), to a single-phase (dry) gas CBM well in the Arkoma Basin, and to a "dewatered" CBM well in the Raton Basin. In both cases, relative permeability effects appeared to be negligible, and there was no mention of stress- or desorption-dependent permeability, multi-layer effects or other reservoir complexities. Mohaghegh and Ertekin[13] generated type-curves using a numerical simulator, and assumed a constant pressure inner boundary condition. To the authors' knowledge, this was the first attempt to incorporate two-phase reservoir characteristics and desorption characteristics into CBM production type-curve analysis. Other complex reservoir behavior was not addressed. Unique type-curve sets are required for differing degrees of drawdown and initial water saturations. Aminian *et al.*[14-15] also generated type-curves using a numerical simulator, and defined a new set of dimensionless variables. The type-curves were demonstrated to be sensitive to isotherm parameter assumptions, flowing pressure and relative permeability. Clarkson *et al.*[16] focused upon single-phase CBM well production, and adapted existing techniques such as Fetkovich type-curves, PTA and FMB, and addressed additional complex reservoir behavior such as multi-layer effects and permeability anisotropy. Jordan *et al.*[17] similarly applied advanced CBM PDA techniques (type-curves + FMB) to simulated single-phase CBM well production, and introduced the idea of including changing effective permeability, such as is the case for two-phase CBM wells, into the FMB methodology. Both the Clarkson *et al.*[16] and Jordan *et al.*[17] studies mention that modified pseudotime and material balance pseudotime (including equilibrium desorption effects) and CBM material balance techniques are required in the application of advanced PDA for single-phase CBM reservoirs.

The present work focuses on the extension of existing production data analysis techniques (ex. FMB) to include more complex CBM reservoir behavior such as changes in effective permeability to gas (due to relative permeability and/or absolute permeability) and evolution of produced gas compositions during depletion.

Production Data Analysis Techniques – Theory and Methodology

Coal reservoir properties are complex and often evolve during the process of depleting the reservoir. The discussion thus begins with how the authors have historically estimated critical CBM reservoir parameters, and their changes during fluid production, from field and laboratory data. Not all coal reservoir properties are discussed, just those that are considered essential to account for when using modern PDA, such as effective permeability, relative permeability and adsorption. The reader is referred to the excellent Gas Research Institute publications for additional information on CBM reservoir property evaluation[18-20]. The discussion then focuses on how to incorporate these unique CBM reservoir properties into modern production data analysis techniques such as FMB and type-curve analysis. As will be shown later with simulated and field examples, these techniques may be used in parallel, along with analytical reservoir simulation, to yield a more complete reservoir description.

Effective Permeability Changes During Depletion. The effective permeability to gas in CBM reservoirs may evolve during depletion due to relative permeability changes as water saturations decrease in two-phase (gas+water) reservoirs[19], due to absolute permeability loss as a function of effective stress changes, or due to absolute permeability gain as a function of gas desorption ("matrix-shrinkage") effects[21]. In the prolific Fruitland Coal "Fairway" CBM play of the San Juan Basin, for example, both relative permeability and absolute permeability effects are known to occur[22], but are difficult to isolate using commonly gathered field data (production+flowing pressures).

Recently, the authors (see Clarkson and McGovern[23], and independently Gierhart *et al.*[24]), developed a simple methodology to estimate the trend of effective permeability to gas growth as a function of depletion for Fruitland Coal Fairway wells. The methodology involves the approximation of the effective permeability to gas (k_g) using Darcy's law, gas production rates, accurately measured (or estimated) flowing and shut-in pressures. The radial form of Darcy's law (using gas-phase pseudopressure) for pseudosteady-state radial flow was used as a starting point:

$$q_g = \frac{7.03x10^{-4} k_{rg} kh\left[m(p_R) - m(p_{wf})\right]}{T\left[\ln(r_e / r_w) - 0.75 + s + Dq_g\right]} \quad \text{.....(1)}$$

Note that the standard conditions of 14.7 psia and 60°F are assumed in the constant $7.03x10^{-4}$ and q_g has the units of Mscf/D.

Using gas flow rates, and estimated flowing and shut-in pressures (converted to pseudopressure using gas-phase properties as a function of pressure, temperature and composition), one can solve for the term outside of the pseudopressure drop as follows:

$$\frac{q_g}{\left[m(p_R) - m(p_{wf})\right]} = \frac{7.03x10^{-4} k_{rg} kh}{T\left[\ln(r_e / r_w) - 0.75 + s + Dq_g\right]} \quad \text{.....(2)}$$

The trend observed in the left-hand-side of Eq. 2 is assumed to be primarily a function of changes in $k_g = k_{rg}*k$. It is assumed that the reservoir is a single-layer, is homogenous and isotropic and that skin (s), drainage radius (r_e), net pay (h) and non-Darcy effects (Dq_g) are constant during depletion. Note that if independent estimates of these parameters are available during the production period, they may be used to

improve the analysis. With assumed values of skin, net pay and drainage area, Eq. 2 may be solved for k_g:

$$k_g = \frac{q_g T\left[\ln\left(r_e / r_w\right) - 0.75 + s + Dq_g\right]}{7.03x10^{-4} h\left[m(p_R) - m(p_{wf})\right]} \quad (3)$$

This methodology does not isolate the effects of relative permeability and absolute permeability changes. The resulting trend in k_g as a function of pressure has been demonstrated to be exponential in form by Clarkson and McGovern[23] for coals in the Fruitland Coal Fairway. Independently, Gierhart *et al.*[24] observed that the performance coefficient *C*, calculated using the back-pressure equation, exhibited an exponential growth with a decrease in reservoir pressure, which they interpreted to be mainly due to absolute permeability growth associated with matrix-shrinkage (see **Fig. 1**). This exponential trend may not necessarily occur outside of the Fairway, or in other basins, so caution must be used in extrapolating these trends.

It is worth mentioning that the analytical models that have been developed to account for the effects of stress and desorption upon absolute permeability may also be used to model field data (ex. using the Palmer-Mansoori model[21]), but these models require a variety of rock mechanical and reservoir properties that may not be known *a-priori*. Further, it is necessary to couple these models with relative permeability estimates for two-phase reservoirs, during the early dewatering phase, which may not be straight forward.

Relative permeability effects for CBM reservoirs has received little attention in recent years, although carefully-determined experimental data was published by Gash *et al.*[25] in the early 1990's. These authors have found that field-derived 'pseudo relative permeability' curves work well in simulator history-matching efforts in the Fruitland Coal Fairway of the San Juan Basin, requiring little to no "tweaking". In the generation of these curves, it was assumed that relative permeability effects dominated the effective permeability to gas growth at higher reservoir pressures (> 600 psia), and that absolute permeability growth dominated at lower pressures, when water saturations were changing slowly. Fetkovich *et al.*[26] and Fraim and Wattenbarger[27] have found that pseudo relative permeability curves derived for volatile oil and solution gas reservoirs look quite different from core-derived data, which can also be expected for CBM reservoirs.

One simple method that can be used to derive pseudo relative permeability curves for CBM reservoirs is described in Appendix A. As with the k_g – growth method described above, our derivation of pseudo relative permeability curves does not separate out other complex reservoir behavior; for example the fracture pore volume, which affects phase saturations and base absolute permeability is likely to evolve at all stages of depletion. The authors have not applied this method to areas outside the Fruitland Coal Fairway, or outside San Juan Basin, leaving its universal applicability in question.

Multi-component Adsorption. Much literature has been dedicated to the experimental determination and modeling of equilibrium single and multi-component gaseous adsorption on coal due to the fact that adsorption is the dominant storage mechanism for CBM reservoirs. Adsorption isotherm model parameters, such as those obtained using the popular Langmuir adsorption isotherm, are required as input to the currently-available CBM material balance equations[28-32]. CBM material balance calculations are in turn required for application of modern PDA techniques to CBM reservoirs, as described below. In some cases, where produced gases are composed primarily of one component, it is only necessary to account for the adsorption of a single gas component, corrected to in-situ conditions (at average composition of reservoir). Where multi-component gases exist in the reservoir, the relative adsorption of the primary components must be taken into account and modeled for accurate material balance calculations[28]. Further, the produced gas composition may change during depletion (see **Fig. 2a** for example), primarily due to relative adsorption effects and the difference in diffusion times of the components[33]. The evolving produced gas composition, where sorption times are small, may be estimated using multi-component adsorption models (assuming equilibrium conditions exist), which usually require as input the single component isotherm parameters. It is important that the composite isotherm resulting from the match of produced gas compositions is used in the material balance calculations, as demonstrated in later examples.

The two methods used by the authors to model produced gas compositions in the field are those due to Harpalani and Pariti[34] (HP) and the Extended Langmuir[19] (EL) method. Both of these methods, described in Appendix B, were chosen because of their analytical simplicity, although more rigorous, and in some cases more accurate, multi-component adsorption models exist in the literature[35-36]. The applications described below are for a binary gas of methane and carbon dioxide, although multi-component gases may also be treated.

Limited comparisons have been made between the HP and EL approaches for modeling free-gas compositions, in equilibrium with multi-component adsorbed gases. Harpalani and Pariti[34] noted that the EL approach was slightly more accurate for predicting binary gas adsorption, determined in the laboratory. These authors have used the two approaches to model produced gas compositions in the field, assuming the produced gas is representative of the free gas in equilibrium with the adsorbed gas. An example comparison is shown in **Fig. 2b** for a binary adsorbed gas mixture of methane and carbon dioxide, which is common in the Fruitland Coal Fairway. The two approaches generally give similar results at high pressures (using the same inputs), but tend to diverge at low pressures. Additional comparisons using field data, are planned for the future. The HP approach was used in the field example given below, for produced gas containing a binary mixture of gases.

Flowing Material Balance. The flowing material balance (FMB) method[9-10], has become a popular technique for determining original-gas-in-place in the absence of shut-in pressures (but requiring flowing pressure data), once a well has reached boundary-dominated flow. The derivation of the FMB starts with the solution to the diffusivity equation during boundary-dominated flow; we discuss various forms of the diffusivity equation for CBM and the derivation of the FMB equation in Appendix C for completeness.

In previous work[16], it was demonstrated that this method could be applied to single-phase (gas) CBM reservoirs, in the absence of complex reservoir behavior (multi-layer, absolute permeability growth etc.), by accounting for equilibrium (or instantaneous) desorption of gas during depletion. Desorption is included in the total compressibility term ("desorption compressibility", see Appendix C). We first start with a discussion of the FMB method for single-phase (water or gas) CBM reservoirs, then extend the discussion to include adaptations for two-phase (gas and water) CBM reservoirs and those with changing absolute permeability.

Single-Phase CBM Reservoirs. In some instances, CBM reservoirs may produce mostly water or gas, and hence exhibit single-phase flow characteristics for at least a portion of their producing life. Undersaturated CBM reservoirs will produce mostly water until the desorption pressure is reached, at which point the reservoir will exhibit two-phase flow characteristics. If a well has reached boundary-dominated flow while still above the desorption pressure, there may be an opportunity to extract drainage area, initial water-in-place, and possibly even estimate absolute permeability (actually effective permeability to water). The FMB equation for a slightly compressible fluid (i.e. water) is[10]:

$$\frac{q_w}{\Delta p} = -\frac{Q_w}{\Delta p c_t}\frac{1}{N_w b_{pss}} + \frac{1}{b_{pss}} \quad \text{.....(4)}$$

where:

$$b_{pss} = \frac{141.2 B_w \mu_w}{kh}\left(\ln\frac{r_e}{r_{wa}} - \frac{3}{4}\right) \quad \text{.....(5)}$$

and:

$$N_w = \frac{7758\phi hA}{B_w} \quad \text{.....(6)}$$

Note that radial flow is assumed, but that non-radial flow may be accounted for through the incorporation of shape factors. During boundary-dominated flow, Eq. 4 represents a straight line as follows:

$$\frac{q_w}{p_i - p_{wf}} = mx + b \quad \text{.....(7)}$$

where:

$$m = \frac{-1}{N_w b_{pss}} \quad \text{.....(8)}$$

$$x = \frac{Q_w}{\Delta p c_t} \quad \text{.....(9)}$$

$$b = \frac{1}{b_{pss}} \quad \text{.....(10)}$$

The original-water-in place may be extracted from the x-intercept, and permeability (absolute if single phase), may be extracted from the y-intercept as follows:

$$k = \frac{141.2 B_w \mu_w}{h}\left(\ln\frac{r_e}{r_{wa}} - \frac{3}{4}\right) * b \quad \text{.....(11)}$$

The FMB, as applied for single-phase, conventional volumetric gas reservoirs, is[10]:

$$\frac{q_g}{m(p_i) - m(p_{wf})} = \frac{-2 q_g t_{ca} p_i}{\left[m(p_i) - m(p_{wf})\right] * \left[\mu_g c_t Z\right]_i}\frac{1}{G_i b'_{pss}} + \frac{1}{b'_{pss}} \quad \text{...(12)}$$

where:

$$b'_{pss} = \frac{1.417 x 10^6 T}{kh}\left(\ln\frac{r_e}{r_{wa}} - \frac{3}{4}\right) \quad \text{.....(13)}$$

During boundary-dominated flow, Eq. 12 represents a straight line as follows:

$$\frac{q_g}{m(p_i) - m(p_{wf})} = mx + b \quad \text{.....(14)}$$

where:

$$m = \frac{-1}{G_i b'_{pss}} \quad \text{.....(15)}$$

$$x = \frac{2 q_g t_{ca} p_i}{\left[m(p_i) - m(p_{wf})\right] * \left[\mu_g c_t Z\right]_i} \quad \text{.....(16)}$$

$$b = \frac{1}{b'_{pss}} \quad \text{.....(17)}$$

G_i can thus be extracted from the x-intercept. Note that the calculation of G_i requires iteration due to the pressure-dependent properties of the gas as a function of reservoir pressure. In addition to G_i, absolute permeability (k), which is assumed to be constant in this case, may be extracted from the y-intercept of the FMB straight line, using Eq. 13 and 17 as follows:

$$k = \frac{1.417 x 10^6 T}{h}\left(\ln\frac{r_e}{r_{wa}} - \frac{3}{4}\right) * b \quad \text{.....(18)}$$

For a unique k value to be obtained, however, net pay and skin (r_{wa} calculation) must be known, and boundary-dominated flow must have been reached.

For single-phase coal reservoirs exhibiting instantaneous desorption, and that have a static permeability, the FMB may be linearized during boundary-dominated flow by modifying the material balance pseudotime to include the effects of desorption. As discussed previously[16], this is achieved through modification of the total compressibility term to include desorption compressibility[37]. The inclusion of a pseudotime modified for desorption is necessary to linearize the diffusivity equation for CBM reservoirs[12].

An alternative expression for x in Eq. 16 may be obtained by using the definition of t_{ca} by Palacio and Blasingame[7] and Agarwal *et al.*[9]:

$$t_{ca} = \frac{(\mu_g c_t)_i}{q_g}\int_0^t \frac{q_g\,dt}{\bar{\mu}_g \bar{c}_t} = \frac{(\mu_g c_t Z)_i}{q_g}\frac{G_i}{2p_i}\left[m(p_i) - m(p_R)\right] \text{...(19)}$$

where $\bar{\mu}_g$, $\bar{c}_t$ are calculated at average reservoir pressure.

Note that Palacio and Blasingame[7] used normalized pseudopressure in their definition of material balance pseudotime, whereas Agarwal *et al.*[9] used the pseudopressure as defined by Al-Hussainy *et al.*[38].

Substituting this expression for t_{ca} into Eq. 16 yields:

$$x = G_i \frac{\left[m(p_i) - m(p_R)\right]}{\left[m(p_i) - m(p_{wf})\right]} \text{ ....(20)}$$

The FMB Eq. 12 may be written in the form of a straight line (during boundary-dominated flow) as follows:

$$\frac{q_g}{m(p_i) - m(p_{wf})} = mG_i \frac{\left[m(p_i) - m(p_R)\right]}{\left[m(p_i) - m(p_{wf})\right]} + b \text{ ....(21)}$$

In order to apply Eq. 21 for CBM reservoirs, $m(p_R)$ must be obtained using material balance equations that incorporate desorption effects and G_i must be calculated using the GIP equation for CBM (Eq. C-17). There are currently numerous versions of the material balance equation for CBM, with varying degrees of complexity. If gas composition changes as a function of depletion due to relative adsorption of the gaseous components[33], the composite isotherm resulting from the match of produced gas compositions must also be used in the material balance calculations. This is demonstrated later using Fruitland Coal Fairway examples.

As with the single-phase conventional FMB method, permeability may be estimated for single-phase CBM reservoirs using Eq. 18, provided boundary-dominated flow has been reached and skin and net pay can be estimated. One advantage that the FMB method offers over type-curve analysis for OGIP and permeability estimation (presented previously for single-phase CBM[16]) is that if Eq. 21 is used, and free-gas storage is negligible in Eq. C-17, fracture porosity need not be estimated, and desorption compressibility (Eq. C-8) does not have to be calculated. Estimation of both of these parameters (ϕ and c_d) is required for the type-curve analysis presented previously[16].

Two-Phase CBM Reservoirs. The FMB can be linearized for gas production from two-phase CBM reservoirs during pseudosteady-state flow by replacing absolute permeability with effective permeability to gas in the definition of b'_{pss} where:

$$k_g = k_{rg} k \text{ ....(22)}$$

In our derivations, we have separated k_{rg} from b'_{pss}, keeping the definition of b'_{pss} as given in Eq. 13 and defining the FMB as follows:

$$\frac{q_g}{\left[m(p_i) - m(p_{wf})\right]k_{rg}(S_g)} = \frac{-2q_g t_{ca} p_i}{\left[m(p_i) - m(p_{wf})\right]*\left[\mu_g c_t Z\right]_i}\frac{1}{G_i b'_{pss}} + \frac{1}{b'_{pss}} \text{ ...(23)}$$

The FMB Eq. 23 may be written in the form of a straight line (during boundary-dominated flow) as follows:

$$\frac{q_g}{\left[m(p_i) - m(p_{wf})\right]k_{rg}(S_g)} = mG_i \frac{\left[m(p_i) - m(p_R)\right]}{\left[m(p_i) - m(p_{wf})\right]} + b \text{ ....(24)}$$

The definitions of m and b, as given in Eq. 15 and 17, are preserved, and relative permeability to gas now appears on the left hand side of the equation. Assumptions for this formulation are, in addition to those stated for the single-phase case, that pressure and saturation gradients in the reservoir are minimal, and that relative permeability is known, or can be reasonably approximated and the same relative permeability curve can be applied throughout the drainage volume of the reservoir.

In some cases where saturation and pressure gradients are strong, it may be necessary to include k_{rg} in the definition of pseudopressure, analogous to the approach used for solution-gas drive reservoirs[39]. The FMB equation for gas may be written in the form of a straight line (during boundary-dominated flow) as follows:

$$\frac{q_g}{\left[m^*(p_i) - m^*(p_{wf})\right]} = mG_i \frac{\left[m^*(p_i) - m^*(p_R)\right]}{\left[m^*(p_i) - m^*(p_{wf})\right]} + b \text{ ....(25)}$$

Where $m^*(p)$ is the pseudopressure accounting for relative permeability as a function of pressure. $m^*(p)$, which is the modified pseudopressure for gas, is defined as follows:

$$m^*(p) = 2\int_{p_b}^{p} \frac{p k_{rg}(p)}{\mu_g Z} dp \text{ ....(26)}$$

This form of the FMB assumes that the production of the well is dominated by gas which is reasonable assumption for some saturated CBM reservoirs.

In order to use Eq. 25 and 26, a relationship between relative permeability and pressure must be established to

perform the pseudopressure calculation. Following the work of Raghavan[39] for solution-gas reservoirs, the producing gas-water ratio (GWR) was used to calculate the relative permeability ratio (gas to water) as follows (ignoring solution gas):

$$\frac{k_{rg}}{k_{rw}} = \frac{\left(\frac{1{,}000 q_g}{5.6146}\right)\mu_g B_g}{q_w \mu_w B_w} \quad \text{.....(27)}$$

In Eq. 27, gas properties are evaluated at the average reservoir pressure.

The water saturation at each GWR, and hence relative permeability ratio, can then be obtained by interpolating between points on the relative permeability curve[40], provided that the relative permeability curves are known. Once water saturation is known, the same table can be used to calculate relative permeability to gas. The next step is to then establish the relationship between water saturation and pressure. In this work, water saturation, as calculated above, is correlated to the average reservoir pressure obtained from reservoir simulation or from CBM material balance equations. This same curve is assumed to apply to flowing sandface pressure as well.

CBM Reservoirs with Absolute Permeability Growth. A similar approach to that taken for two-phase coal may be used for the case of absolute permeability growth. However, in the case of two-phase CBM reservoirs, absolute permeability growth effects may be difficult to separate out from relative permeability growth. In these cases, we have chosen to establish effective permeability growth as a function of pressure, using the procedure discussed in the section "Effective Permeability Changes During Depletion", and modified the FMB (for gas) in the following manner:

$$\frac{q_g}{\left[m(p_i)-m(p_{wf})\right]k_g(p_R)} = \frac{-2q_g t_{ca} p_i}{\left[m(p_i)-m(p_{wf})\right]^*\left[\mu_g c_t Z\right]_i}\frac{1}{G_i b^*_{pss}} + \frac{1}{b^*_{pss}} \text{.(28)}$$

where:

$$b^*_{pss} = \frac{1.417x10^6 T}{h}\left(\ln\frac{r_e}{r_{wa}} - 0.75\right) \quad \text{.....(29)}$$

Eq. 28 then becomes:

$$\frac{q_g}{\left[m(p_i)-m(p_{wf})\right]k_g(p_R)} = m\frac{G_i\left[m(p_i)-m(p_R)\right]}{\left[m(p_i)-m(p_{wf})\right]} + b \text{.....(30)}$$

The k_g can therefore be extracted from the y-intercept during boundary-dominated flow, and not absolute permeability.

Production Type-Curve Analysis. A previous paper[16], along with other published works[11,13-15], addressed the application of production type-curves to CBM production data. This subject will not be discussed in detail in the current work, but some additional comments will be made regarding the use of different time functions.

In Ref. 16, the authors discussed how to modify the classic Fetkovich type-curves to analyze single-phase CBM production by simply including desorption compressibility (Eq. C-8) in the definition of the dimensionless time function (Eq. D-3). Real time was used in the calculation of dimensionless time, consistent with the original Fetkovich work[1]. Modern production type-curve analysis makes use of rate-normalization (pressure or pseudopressure drop normalized rate) techniques and material balance pseudotime (Eq. 19) to account for changing operating conditions and gas property variation as a function of pressure. For CBM reservoirs, as discussed previously[16], material balance pseudotime must also account for CBM storage through adsorption.

It is therefore possible to use modern production type-curve analysis techniques for single-phase (gas) CBM reservoirs, with a modified definition of material balance pseudotime for CBM, just as has been shown for FMB. Using the Fetkovich type-curves as an example, (the other available production type-curves may be similarly treated), the dimensionless time variable is re-cast in terms of material balance pseudotime (Eq. D-3) as well as the extracted reservoir and stimulation variables from the type-curve match (Eq. D-6, D-9 and D-10). Use of material balance pseudotime forces the depletion to follow a harmonic stem[7], as opposed to an exponential stem if pseudotime is used[4]. An example is given in **Fig. 3**; the numerically-generated single-phase CBM example provided in Ref. 16, originally analyzed using the Fetkovich curves without material balance pseudotime, is reproduced using the modified Fetkovitch type-curves (with material balance pseudotime). Fig. 3a illustrates the type-curve match using real time in the definition of dimensionless time (Eq. D-3), and Fig. 3b illustrates the use of material balance pseudotime. The result of the transformation, is that depletion now follows a harmonic stem Fig. 3b, and the analytical method for calculating GIP provided by Palacio and Blasingame[7] may be used (Eq. D-12) to extract GIP associated with the fracture pore volume from the match. This GIP, with knowledge of fracture porosity and initial formation volume factor, may then be converted to a bulk volume estimate for adsorbed gas GIP estimates. Alternatively, Eq. D-10 may be used to calculate bulk volume directly, which can then be used to estimate adsorbed gas GIP, as discussed previously[16]. The type-curve match, shown in Fig. 3b, resulted in estimates of reservoir and skin variables similar to the original analysis using real time instead of material balance pseudotime.

It is important to note that in the case of undersaturated CBM reservoirs, which produce primarily water initially, the type-curves and FMB techniques may be used to analyze the water production data, in an analogous fashion to oil production from undersaturated oil reservoirs. If the production is truly single phase, relative permeability effects need not be accounted for and pseudotime calculations are not required. Provided accurate flowing pressure and water production data, these techniques may be used to extract important reservoir information such as drainage area, effective permeability to water (often used as a proxy for absolute permeability for CBM reservoirs) and skin.

Example Applications

Single-Phase (Gas) CBM Well. This Horseshoe Canyon CBM well was examined previously[16] using the Fetkovich type-curves, flowing material balance and analytical simulation. The modified (for single-phase CBM) type-curves were demonstrated to yield permeability and skin estimates similar to the initial well test performed on the well. The FMB analysis (which incorporated desorption effects) yielded a GIP similar to the type-curve analysis. The analysis was then confirmed through the use of an analytical simulator (also CBM-specific) to history-match the well production. The input reservoir data is re-produced in Table 1. Sorption times are assumed to be negligible (instantaneous desorption).

This example is re-presented to demonstrate how FMB can be used as a method to estimate permeability, if the skin is known or can be reasonably estimated. We also show how FMB can be used as a diagnostics tool. To illustrate this, the well production data, and the analytical simulator match to the data, are re-cast in FMB coordinates (normalized rate and normalized cumulative production), shown in **Fig. 4a**. A straight line is also fit to the production data (**Fig. 4b**), which can be used to estimate OGIP and permeability (if skin is known), using Eq. 15, 17, 18. The skin was obtained from the initial well test (0.2); the straight line fit therefore yields an OGIP estimate of ~ 150 MMscf, and a permeability of 9.1 md. These numbers are consistent with the previous analysis[16]. If the skin were not known from well-test, the value could have reasonably estimated as having values between 0 and +1, consistent with the completion methodology. This range would yield a permeability range from 8.8 – 10.0 md. Note that in this example, we have assumed static permeability and skin, and that desorption is instantaneous.

The FMB can be used as a diagnostic tool as well, to examine flow regimes and changes in well productivity. The early time production of this well (normalized cumulative production < 10) is non-linear on the FMB, an indication of transient flow behavior. The early-time simulator production profile (Fig. 4b) also shows transient flow characteristics, and the fit of the simulated production to actual data during this time period may be an indicator of the reasonableness of the permeability/skin combination. The FMB at later times appears to become linear, an indication of boundary-dominated flow. There do not appear to be any significant productivity issues with this well, which may cause a divergence of the production from the straight line on the FMB.

Single-Phase (Water) CBM Well. Undersaturated CBM reservoirs may produce mainly water for a substantial period of time, prior to desorption pressure being reached. Some gas saturation is likely to develop near wellbore, if the well is drawn down enough to cause desorption in the near wellbore-area. It may be possible, however, that quantitative information about water-in-place, drainage area and absolute permeability (or effective permeability to water at near 100% water saturation) can be extracted from the FMB or type-curves, provided boundary-dominated flow is reached before the substantial gas saturation is developed. To test this concept, a numerical simulator (single-layer, radial model) was used to generate a production profile for an undersaturated CBM reservoir, assuming a constant water production rate of 35 STB/D, followed by a constant flowing bottomhole pressure constraint of 25 psia. Other relevant simulator inputs are given in Table 2. The relative permeability curves used in the simulation are given in **Fig. 5a** and simulated gas, water, and flowing (bottomhole) pressure profiles are given in **Fig 5b**.

The first 200 days of water production, plotted in FMB coordinates, is given in **Fig. 6a**. A transient (non-linear on plot) flow period is noticeable early on, followed by a straight-line segment during boundary-dominated flow. Once a significant gas saturation develops, the plot then becomes non-linear (not shown). A straight-line fit to the boundary-dominated flow period data yields an original water-in-place number (~98,000 STB) very similar to the simulator-calculated value (~96,000 STB). Permeability (with skin assumed = 0) is also close to the simulator input value (5 md).

A Fetkovich type-curve match (using r_e / r_{wa} stem = 5000), using rate-normalization to account for declining back-pressure, is shown in **Fig. 6b**. The extracted permeability and skin (5.1 md and 0.17) are reasonably close to the simulator input values (5 md and 0). Note the calculations provided by Fetkovich[1] for a liquid were used.

Two-Phase (Gas+Water) CBM Well. In this example, numerically simulated production was analyzed using the two-phase version of the FMB equation (Eq. 24, 25). The simulated example is similar to that used by Seidle[41], with most reservoir properties typical of those expected for Powder River Basin CBM reservoirs. Relevant simulation parameters are given in Table 3. As with the Seidle[41], straight line relative permeability curves were assumed (**Fig. 7a**), and a single-layer, radial simulation grid was used (60 radial grid-blocks, spaced logarithmically). The water production rate was specified at 400 STB/D, followed by a constant flowing bottomhole pressure constraint of 25 psia. The gas and water production rates, shown in **Fig. 7b**, are similar, but do not exactly correspond to those given by Seidle[41], likely due to some fluid property assumptions not specified in the original work. A sorption time of 2 days was assumed in this work.

In order to apply the FMB equation to the simulation data, S_w must first be calculated, then used to establish relative permeability to gas. In this work, the k_{rg}/k_{rw} was calculated using gas and water production data and Eq. 27. S_w, corresponding to each k_{rg}/k_{rw} point, was then obtained from a look-up table containing relative permeability data (k_{rg}, k_{rw}, k_{rg}/k_{rw} and S_w). k_{rg} is therefore also established from the lookup table once S_w is known. S_w calculated in this way is lower than the pore-volume average calculated with the simulator, and is therefore less than would be expected from a CBM material balance equation. The S_w is some value between that near wellbore and the pore-volume average.

Assuming saturation gradients are negligible, we first plotted the normalized rate (left hand side of Eq. 24) vs. normalized cumulative production (Eq. 20) in **Fig. 8a**. We used the first thousand days of simulation data only, and the simulator pore-volume average pressure in the calculations (note that CBM material balance equations may also be used to calculate p_R). After a brief transient flow period (non-linear

portion of the plot), the data becomes linear during the boundary-dominated flow period. Use of normalized gas rate containing k_{rg} therefore linearized the FMB plot during boundary-dominated flow period, as expected. Fitting a straight line to the boundary-dominated flow portion of the data allowed OGIP and k (assuming skin) to be calculated from the slope and intercept using Eq. 15, 17, 18. The extracted OGIP (351 MMscf) is close to the numerical model-calculated value of 340 MMscf. The extracted permeability (~113 md), however, is about 13% too high. This is most likely caused by the assumption that saturation gradients are negligible, and that k_{rg} is uniform throughout the drainage volume at each time-step.

The next step was to apply the more rigorous FMB that incorporates relative permeability calculations in the definition of pseudopressure (Eq. 26). In order to incorporate k_{rg} into the pseudopressure calculation, a correlation between S_w and pressure is required. In this work, we chose to correlate S_w to the pore-volume average pressure calculated from the simulation model (**Fig. 9**). This correlation was used in both the $m(p_R)$ and $m(p_{wf})$ calculations, which assumes the S_w vs. pressure correlation is the same throughout the drainage volume of the reservoir, which must be considered an approximation. Once this correlation is established, Eq. 26 may be used to calculate pseudopressure for gas at the two pressure levels (flowing sandface and reservoir pressure).

Plotting the simulation data in terms of normalized rate vs. normalized cumulative production (with pseudopressure accounting for relative permeability effects) yields a straight line during boundary-dominated flow as before (**Fig. 8b**). This time, a straight line fit through the boundary-dominated flow portion of the plot yields the same permeability value (100 md) as the value input into the simulator (100 md).

A brief sensitivity study was performed to assess the impact of relative permeability assumptions upon the OGIP and permeability estimation from FMB. **Fig. 10a** shows the FMB of the simulator data for this two-phase coal example when no relative permeability effects are incorporated (left hand side of Eq. 12, which assumes single-phase gas production). The plot shows non-linearity late in time, in addition to the early-time non-linearity associated with transient flow. Fitting a straight line through the data results in an OGIP estimate that is substantially different than actual value (450 vs. 340 MMscf), and a permeability that is substantially lower than the actual value (7.9 vs. 100 md). The calculated permeability is, however, reasonably close to the effective permeability value ($k_{rg}*k$) at the start of boundary dominated flow. If the incorrect relative permeability curve is assumed, as is shown in **Fig. 10b**, where the gas relative permeability curve used in the FMB calculations is similar to the Gash *et al.*[25] curves (Fig. 5a), the FMB plot is again non-linear in later boundary-dominated flow. If a straight line is fit to the linear portion of the FMB plot, the resulting OGIP is reasonably close to the actual value (319 MMscf vs. 340 MMscf), but the calculated permeability is much higher than actual (610 md vs. 100 md), reflecting the error in relative permeability assumptions.

One of the problems encountered in commercial two-phase CBM reservoirs is the inability to separate out the effects of relative permeability and absolute permeability effects during the early dewatering stage using only commonly-gathered field data, such as flowing pressures and production data. We have therefore chosen not to isolate these effects, as discussed in the next example.

Two-Phase CBM Well with Absolute Permeability Growth. For Fruitland Coal Fairway wells exhibiting absolute permeability growth due to matrix-shrinkage effects, relative permeability changes, and evolution of produced (binary) gas composition, we have developed the following procedure to history-match single-well data:

1) Use an analytical simulator or appropriate CBM material balance equation to match historical shut-in pressures (or offset pressure-observation well pressures if available).
2) If the well has historical produced gas composition data, and the gas composition evolves during depletion, use either the Harpalani and Pariti[34] or Extended Langmuir methods (see Appendix B) to match the gas compositions as a function of shut-in pressure. Ensure the single-component isotherm data yield a composite isotherm data that is consistent with composite isotherm used for model match in step 1. If not, iterate steps 1 and 2 until the same composite isotherm results.
3) Calculate the k_g – growth from field data and the modeled reservoir pressures using Eq. 3. Fit a curve to the k_g – growth vs. reservoir pressure data. For Fairway Fruitland Coal wells, an exponential growth curve appears to work best in most cases. The fitted curve is then used in the analytical simulator to calculate productivity increases as a function of depletion.
4) Observe flowing material balance plot to note productivity variation (model to actual).
5) Adjust model k_g curve if necessary to match flowing pressure data.

Two Fairway Fruitland Coal examples are provided in **Fig. 11-15**. Well 1 (Fig. 11a) has mostly monthly production data, until late time where daily production data were available; offsets two pressure observation wells that serve as a continuous monitor of reservoir pressure near the producing well; and was sampled periodically for produced gas composition. Although flowing pressure estimates (calculated from wellhead pressures) were available for this well, the pressure data set was not complete for the entire history of the well; the flowing pressures had, however, been closely matched during a reservoir simulation study of the area, which modeled the entire well history, and it is the simulated flowing bottomhole pressure data that is used in this example.

Gas production rate for well 1 (Fig. 11a) exhibits a classic early-time "negative" decline, for the first 2 years of production, associated with dewatering of the coals and increases in effective permeability to gas. The gas composition of the well is primarily composed of methane and carbon dioxide, with the latter increasing during depletion as a result of relative adsorption effects. A match of the produced CO_2 concentration, using the Harpalani and Pariti[34] method, and the resulting composite isotherm is shown in Fig. 12. This composite isotherm was then used in the history-match of offset pressure observation well, assumed to be a reasonable

proxy for reservoir pressure (Fig. 12c). The match assumes that the well drains a 320-acre drainage radius, which is consistent with the offset well spacing. Once the reservoir pressure match was obtained, a plot of k_g versus simulated reservoir pressure was created (Fig. 13a). The k_g – growth curve is exponential, as expected for Fairway wells in this area. An exponential line was then fit to the k_g – growth plot, and was used in the analytical model to calculate productivity increases as a function of depletion. The robustness of the assumed productivity increase is best viewed when the field and simulator data are plotted in FMB coordinates, with the left-hand-side of Eq. 28 plotted versus normalized cumulative production. In the FMB plot (Fig. 13b) the variance of the actual productivity to the model productivity becomes clearer; at early times (normalized cumulative production < 5 bcf), the model is over-predicting productivity relative to the field data, and at late times, the two converge. The flowing pressure match (Fig. 13c) using the analytical model, with the exponential k_g – growth curve included, is quite good, despite some productivity variance.

The same procedure was used for well 2 (Fig. 14-15), but in this case, daily data was available for the entire well history. This well is also offset by a pressure observation well. The match of produced CO_2 concentration (Fig. 14b) resulted in a composite isotherm that was used in the history-match of POW pressure (Fig. 14c). The k_g – growth plot versus model reservoir pressure and FMB plots are given in Fig. 15a and 15b, respectively. k_g again appears to follow an exponential trend, which was fit with a straight line on the semi-log plot for the model calculations. Data scatter is more evident in this example than the previous example; no attempt was made to filter the data to remove anomalous points. Despite the scatter, clear trends in the data exist; there is one section of data that has an incorrect flowing bottomhole pressure estimate (just below 800 psia, Fig. 15a) due to a switch in flowing configuration, resulting in an artificially high k_g estimate. The middle region of the FMB plot shows a dip in normalized rate, which may also be due to an incorrect estimate of p_{wf}. The flowing pressure match (Fig. 15c), however, appears quite good through most of the well life, indicating that the k_g – growth curve that is used in the model is reasonable.

Discussion

In this work, the authors have attempted to apply advanced production data analysis techniques to CBM wells (actual and synthetic) completed in reservoirs exhibiting effective permeability growth to gas (due to relative permeability and absolute permeability growth). Although we have been successful with the simulated and field examples provided in this work, we believe more work is required to refine the techniques, particularly for two-phase flow.

For two-phase CBM, a methodology was introduced to linearize the FMB equation, using field data to approximate water saturations. In order to use this approach, relative permeability curves must be derived or inferred. The authors have provided a method for developing pseudo relative permeability curves from field data, assuming a single-layer, homogeneous reservoir (Appendix A). In reality, multi-layer, heterogeneous coals may be more typical in the field. Fraim and Wattenbarger[27] illustrate how vertical and horizontal permeability variation with crossflow causes pseudo relative permeability curves to become rate-path dependent for solution gas drive reservoirs. These effects could also be important for CBM reservoirs exhibiting multi-layer characteristics. Future work will discuss in detail how to adapt the single-layer analysis methods discussed in this work to multi-layered reservoirs.

The authors have not applied the two-phase FMB method using actual field data, therefore the results must be viewed as preliminary. The technique is designed to utilize production data to establish S_w and is therefore contingent on the quality of reported water production (not always as accurate as the saleable commodity, gas) and requires that p_R be estimated from field data or material balance. S_w may also be estimated from material balance[30-32], but the value may differ from that using the procedure described in this work. The authors continue to explore different methods for calculating S_w.

An additional problem with the two-phase method, using the modified pseudopressure function (Eq. 26), is the need to correlate relative permeability to pressure. A simple method is introduced to correlate water saturation to volumetric average pressure; in the simulated example provided, this method provided accurate estimates of OGIP and absolute permeability. Limited additional simulated examples over a range of reservoir properties yielded similar results (not shown). We continue to investigate the range of applicability of this method.

The use of modified desorption compressibility is necessary to linearize the various forms of the diffusivity equation provided for CBM reservoirs (for single-phase gas or saturated reservoirs with instantaneous desorption). This additional compressibility can be incorporated into a modified pseudotime or material balance pseudotime term so that modern methods of production data analysis may be used for CBM reservoirs, if desorption is assumed to be instantaneous. We have mainly discussed the application of three PDA techniques: FMB, Fetkovich type-curve analysis, and analytical simulation. Other type-curves (ex. Blasingame[7], Agarwal-Gardner[9] etc.), may be similarly used to yield quantitative information from CBM reservoirs, provided the modifications discussed in this work are used.

Conclusions

This paper discusses the application of production data analysis techniques, such as FMB and type-curve analysis, to single-phase (gas or water) and two-phase (gas+water) CBM wells. The major conclusions are:

1) The flowing material balance technique can be modified to account for complex CBM reservoir behavior such as two-phase flow and effective permeability changes during depletion as a function of absolute and relative permeability effects.
2) Single-phase gas production from CBM reservoirs can be analyzed using single-phase FMB and type-curve analysis techniques and used to extract quantitative estimates of permeability (if skin is known) and gas-in-place.
3) FMB can be used as a diagnostic tool, when coupled with analytical simulation, to examine productivity changes during depletion.

4) Single-phase water production from undersaturated CBM reservoirs can be analyzed using single-phase FMB and type-curve analysis techniques and used to extract quantitative estimates of permeability (if skin is known) and water-in-place, provided relative permeability effects are negligible.
5) Two-phase (gas+water) CBM wells can be analyzed using a modified FMB technique, provided that k_{rg}/k_{rw} can be reliably extracted using production data, S_w can be extracted from a known relative permeability curve, and S_w can be related to pressure for rigorous pseudopressure calculations. The techniques provided in this work are adequate for the examples studied, but require further testing to determine their applicability to wider range of CBM reservoir properties.
6) Relative permeability curves, and effective permeability to gas growth, as a function of depletion, may be approximated using field data (fluid production rates, flowing and shut-in pressures).
7) If produced gas compositions change as a function of depletion due to relative adsorption effects, the compositional changes may be modeled using a variety of techniques (we have used the Extended Langmuir equation and a technique provided by Harpalani and Pariti[34] for this purpose). The resulting composite isotherm can then be used for material balance or simulation studies.
8) Fairway Fruitland Coal wells can be analyzed rigorously using FMB combined with analytical simulation provided the effects of effective permeability growth and gas compositional changes during depletion are accounted for.

As discussed above, further work is required to establish the robustness of our FMB technique for analyzing two-phase CBM reservoirs, and perhaps to modify for certain combinations of reservoir parameters.

All the techniques used in this work assume instantaneous desorption (equilibrium between matrix and fractures) – this is not considered to be a serious limitation in the analysis of long-term production data for most commercial CBM reservoirs. A possibly more serious assumption is that of single-layer reservoir behavior; several of the commercial CBM plays studied by the authors exhibit some form of multi-layer behavior, which can be difficult to analyze using standard production data analysis techniques. This will be the subject of a future paper.

Nomenclature

A = drainage area, acres
B_g = gas formation volume factor, reservoir volume/surface volume
B_w = water formation volume factor, RB/STB
b = y-axis intercept of straight line or Langmuir isotherm parameter ($1/p_L$)
b_{pss} = inverse productivity index for water (Eq. 5), psi/(STB/D)
b'_{pss} = inverse productivity index for gas (Eq. 13), psi^2/(cp*MMscf/D)
b^*_{pss} = constant in Eq. 29
c_d = desorption compressibility, psi^{-1}
c_{eff} = effective compressibility (Eq. C-23), psi^{-1}
c_f = fracture system pore volume or formation compressibility, psi^{-1}
c_g = gas compressibility, psi^{-1}
c_t = total compressibility, psi^{-1}
$\bar{c}_t$ = total compressibility, evaluated at average reservoir pressure, psi^{-1}
C_E = equilibrium adsorbed phase molar concentration, lb-moles/ft^3
D = inertial or turbulent flow factor, D/Mscf
G = gas-in-place, Mscf or MMscf
h = formation thickness, feet
k = absolute permeability, md
k_g = effective permeability to gas, md
k_w = effective permeability to water, md
k_{rg} = relative permeability to gas, dimensionless
k_{rw} = relative permeability to water, dimensionless
m = slope of a straight line
$m(p)$= pseudopressure, psi^2/cp
$m^*(p)$= pseudopressure, modified to include relative permeability (Eq. 26, Eq. C-22)
M_g = molecular weight, lb/lb-moles
N_w = original water-in-place, STB
p = pressure, psia
p_b = reference pressure, psia
p_i = initial pressure, psia
p_L = Langmuir pressure constant, psia
p_{wf} = flowing bottomhole pressure, psia
p_R = volumetric average reservoir pressure, psia
q_g = gas surface flow rate, Mscf/D or MMscf/D
q_w = water surface flow rate, STB/D
Q_w = cumulative water production, STB
r = radius, ft
r_e = drainage radius, ft
r_w = wellbore radius, ft
r_{wa} = effective wellbore radius, ft
s = skin factor, dimensionless
S_g = gas saturation, dimensionless, fraction
S_w = water saturation, dimensionless, fraction
t = time, hours or days
t_a = pseudotime, days
t_c = material balance time, days
t_{ca} = material balance pseudotime, days
t_p = pseudotime (Eq. C-24), days
T = temperature, °R
V = adsorbed gas volume, corrected to in-situ conditions, scf/ton
V_b = bulk volume of the reservoir, ft^3
V_L = Langmuir volume constant, scf/ton
V_p = pore volume of the reservoir, ft^3
$x_{i,j}$ = adsorbed phase mole fraction of component i or j
$y_{i,j}$ = gas phase mole fraction of component i or j
Z = gas-law deviation factor, dimensionless

Greek Symbols

α= unit conversion constant, 6.326 ft^{2}cp/(day md psi)
λ_t = total mobility, md/cp

μ_g = gas viscosity, cp
$\bar{\mu}_g$ = gas viscosity evaluated at average reservoir pressure, cp
μ_w = water viscosity, cp
ϕ = fracture porosity, dimensionless, fraction
ρ_c = coal bulk density, g/cm^3
ρ_g = gas density, lb/ft^3
ρ_w = water density, lb/ft^3

Subscripts
a = pseudo
b = reference
c = material balance
ca = material balance pseudo
d = desorption
D = dimensionless
dD = type-curve dimensionless
eff = effective
E = equilibrium
f = fracture system
g = gas
i = initial or gaseous component
j = gaseous component
L = Langmuir
o = initial
p = pore
pss = pseudosteady-state
rg = relative to gas
rw = relative to water
R = reservoir
sc = standard conditions
t = total
w = water
wa = apparent wellbore
wf = sandface

Superscripts
‘ = dummy variable of integration or altered variable
– = average property
* = altered variable
b = reference

Operators
$d(u)$ = differential in any variable, u
$\partial(u)$ = partial differential
$\Delta(u)$ = change in any variable, u
∇^2 = Laplace operator

Acknowledgments
The authors would like to thank the management of our respective companies for their time to review and permission to publish this paper.

References
1. Fetkovich, M.J.: “Decline Curve Analysis Using Type Curves,” *JPT* (June 1980) 1065.
2. Carter, R.D.: “Type Curves for Finite Radial and Linear Gas-Flow Systems: Constant-Terminal-Pressure Case,” *SPEJ* (October 1985) 719.
3. Fetkovich, M.J. *et al.*: “Decline-Curve Analysis Using Type Curves – Case Histories,” *SPEFE* (December 1987) 637; *Trans.*, AIME, 283.
4. Fraim, M.L., and Wattenbarger, R.A.: “Gas Reservoir Decline-Curve Analysis Using Type Curves With Real Gas Pseudopressure and Normalized Time,” *SPEFE* (December 1987) 671.
5. Blasingame, T.A., Johnstone, J.L., and Lee, W.J.: “Type-Curve Analysis Using the Pressure Integral Method,” paper SPE 18799 presented at the 1989 SPE California Regional Meeting, Bakersfield, California, 5-7 April.
6. Blasingame, T.A., McCray, T.L., and Lee, W.J.: “Decline Curve Analysis for Variable Pressure Drop/Variable Flowrate Systems,” paper SPE 21513 presented at the 1991 SPE Gas Technology Symposium, Houston, Texas, 23-24 January.
7. Palacio, J.C., and Blasingame, T.A.: “Decline-Curve Analysis Using Type Curves—Analysis of Gas Well Production Data,” paper SPE 25909 presented at the 1993 SPE Joint Rocky Mountain Regional and Low Permeability Reservoirs Symposium, Denver, Colorado, 26-28 April.
8. Fetkovich, M.J. *et al.*: “Useful Concepts for Decline-Curve Forecasting, Reserve Estimation, and Analysis,” *SPERE* (February 1996) 13.
9. Agarwal, R.G. *et al.*: Analyzing Well Production Data Using Combined Type Curve and Decline Curve Concepts,” *SPEREE* (October 1999) 478.
10. Mattar, L., and Anderson, D.M.: “A Systematic and Comprehensive Methodology for Advanced Analysis of Production Data,” paper SPE 84472 presented at the 2003 SPE Annual Technical Conference and Exhibition, Denver, Colorado, 5-8 October.
11. Pinzon, C.L., and Patterson, J.: “Production Analysis of Coalbed Wells Using Analytical Transient Solutions,” paper SPE 91447 presented at the 2004 SPE Eastern Regional Meeting, Charleston, West Virginia, 15-17 September.
12. Spivey, J.P., and Semmelbeck, M.E.: “Forecasting Long-Term Gas Production of Dewatered Coal Seams and Fractured Shales,” paper SPE 29580 presented at the 1995 SPE Rocky Mountain Regional/Low-Permeability Reservoirs Symposium, Denver, Colorado, 20-22 March.
13. Mohaghegh, and Ertekin, T.: “Type-Curve Solution for Coal Seam Degasification Wells Producing Under Two-Phase Conditions,” paper SPE 22673 presented at the 1991 SPE Annual Technical Conference and Exhibition, Dallas, Texas, 6-9 October.
14. Aminian, K. *et al.*: “Type Curves for Coalbed Methane Production Prediction,” paper SPE 91482 presented at the 2004 SPE Eastern Regional Meeting, Charleston, West Virginia, 15-17 September.
15. Aminian, K. *et al.*: “Type Curves for Production Prediction and Evaluation of Coalbed Methane Reservoirs,” paper SPE 97957 presented at the 2005 SPE Eastern Regional Meeting, Morgantown, West Virginia, 14-16 September.
16. Clarkson, C.R., Bustin, R.M., and Seidle, J.P.: “Production Data Analysis of Single-Phase (Gas) CBM Wells,” paper SPE 100313 presented at the 2006 SPE Gas Technology Symposium, Calgary, Alberta, 15-17 May.
17. Jordan, C.L., Fenniak, M.J., and C.R. Smith: “Case Studies: A Practical Approach to Gas-Production Analysis and Forecasting,” paper SPE 99351 presented at the 2006 SPE Gas Technology Symposium, Calgary, Alberta, 15-17 May.
18. *Determining Coalbed Gas Content*, J.D. McLennan, P.S. Schafer, and T.J. Pratt (eds.), Gas Research Inst. Report GRI-94/0396, Chicago (1995).

19. Mavor, M.J.: "Coalbed Methane Reservoir Properties," *A Guide to Coalbed Methane Reservoir Engineering*, Gas Research Inst. Report GRI-94/0397, Chicago (1996).
20. *Coalbed Methane Gas-In-Place Analysis*, M. Mavor and C.R. Nelson (eds.), The Gas Research Inst. Report GRI-97/0263, Chicago (1997).
21. Palmer, I., and Mansoori, J.: "How Permeability Depends on Stress and Pore Pressure in Coalbeds: A New Model," paper SPE 36737 presented at the 1996 SPE Annual Technical Conference and Exhibition, Denver, Colorado, 6-9 October.
22. Mavor, M.J., and Vaughn, J.E.: "Increasing Coal Absolute Permeability in the San Juan Basin Fruitland Formation," *SPEREE* (June 1998) 539.
23. Clarkson, C.R. and McGovern, J.M.: "A New Tool for Unconventional Reservoir Exploration and Development Applications," paper 0336 presented at the 2003 Intl. Coalbed Methane Symposium, The U. of Alabama, Tuscaloosa, Alabama, 5-9 May.
24. Gierhart, R., Gips, G., and Seidle, J.: "San Juan Basin Fruitland Coal Pressure Dependent Permeability Observations," presented at the 2006 SPE Applied Technology Workshop on Unconventional Gas, Keystone, Colorado, 19-21 April
25. Gash, B.W., Voltz, R.F., Potter, G., and Corgan, J.M.: "The Effects of Cleat Orientation and Confining Pressure on Cleat Porosity, Permeability and Relative Permeability," paper 9321, presented at the 1993 Intl. Coalbed Methane Symposium, The U. of Alabama, Tuscaloosa, Alabama, 17-21 May.
26. Fetkovich, M.D., Guerrero, E.T., Fetkovich, M.J., and Thomas, L.K.: "Oil and Gas Relative Permeabilities Determined from Rate-Time Performance Data," paper SPE 15431 presented at the 1986 SPE Annual Technical Conference and Exhibition, New Orleans, Lousiana, 5-8 October.
27. Fraim, M.L., and Wattenbarger, R.A.: "Decline Curve Analysis for Multiphase Flow," paper SPE 18274 presented at the 1988 SPE Annual Technical Conference and Exhibition, Houston, Texas, 2-5 October.
28. Jensen, D, and Smith, L.K.: "A Practical Approach to Coalbed Methane Reserve Prediction Using a Modified Material Balance Technique," paper 9765 presented at the 1997 Intl. Coalbed Methane Symposium, The U. of Alabama, Tuscaloosa, Alabama, 12-16 May.
29. Clarkson, C.R., and McGovern, J.M.: "Optimization of Coalbed Methane Reservoir Exploration and Development Strategies Through Integration of Simulation and Economics," *SPEREE* (December 2005) 502.
30. Seidle, J.P.: "A Modified p/Z for Coal Wells," paper SPE 55605 presented at the 1999 SPE Rocky Mountain Regional Meeting, Gillette, Wyoming, 15-18 May.
31. King, G.R.: "Material balance Techniques for Coal-Seam and Devonian Shale Gas Reservoirs with Limited Water Influx," *SPERE* (February 1993) 67.
32. Ahmed, T., Centilmen, A., Roux, B.: "A Generalized Material Balance for Coalbed Methane Reservoirs," paper SPE 102638 presented at the 2006 SPE Annual Technical Conference and Exhibition, San Antonio, Texas, 24-27 September.
33. Cui, X., and Bustin, R.M.: "Controls of Coal Fabric on Coalbed Gas Production and Compositional Shift in both Field Production and Canister Desorption Test," *SPEJ* (March 2006).
34. Harpalani, S., and Pariti, U.M.: "Study of Coal Sorption Isotherms Using A Multi-component Gas Mixture," paper 9356 presented at the 1993 Intl. Coalbed Methane Symposium, The U. of Alabama, Tuscaloosa, Alabama, 17-21 May.
35. Hall, F.E., Zhou, Z., Gasem, K.A.M, Robinson, R.L., Yee, D.: "Adsorption of Pure Methane, Nitrogen, and Carbon Dioxide and Their Binary Mixtures on Wet Fruitland Coal," paper SPE 29194 presented at the 1994 Eastern Regional Conference, Charleston, West Virginia, 8-10 November.
36. Clarkson, C.R." "Application of a New Multi-component Gas Adsorption Model to Coal Gas Systems," *SPEJ* (September 2003).
37. Bumb, A.C., and McKee, C.R.: "Gas-Well Testing in the Presence of Desorption for Coalbed Methane and Devonian Shale," *SPEFE* (March 1988), 179.
38. Al-Hussainy, R., Ramey, H.J. Jr., and Crawford, P.B.: "The Flow of Real Gases Through Porous Media," *JPT* (May 1966), 624; *Trans.*, AIME, 237.
39. Raghavan, R.: "Well-Test Analysis: Wells Producing by Solution Gas Drive," *SPEJ* (August 1976), 196.
40. Mavor, M.J.and Saulsberry, J.L.: "Testing Coalbed Methane Wells," *A Guide to Coalbed Methane Reservoir Engineering*, Gas Research Inst. Report GRI-94/0397, Chicago (1996).
41. Seidle, J. : "Coal Well Decline Behavior and Drainage Areas: Theory and Practice," paper SPE 75519 presented at the 2002 SPE Gas Technology Symposium, Calgary, Alberta, 30 April – 2 May.
42. Lee, J., Rollins, J.B. and Spivey, J.P.: *Pressure Transient Testing*, Textbook Series, SPE, Richardson, Texas (2003), **9**.
43. King, G.R., and Ertekin, T: "State-of-the-Art Modeling for Unconventional Gas Recovery, Part II: Recent Developments (1989-1994)," paper SPE 29575 presented at the 1995 Rocky Mountain Regional/Low-Permeability Reservoirs Symposium, Denver, Colorado, 20-22 March.
44. Kamal, M.M., and Six, J.L.: "Pressure Transient Testing of Methane Producing Coalbeds," paper SPE 19789 presented at the 1989 Annual Technical Conference and Exhibition, San Antonio, Texas, 8-11 October.

Appendix A

A simple method for deriving pseudo relative permeability curves from two-phase (gas and water) CBM reservoirs, analogous to the method outlined by Fetkovich *et al.*[26], is described as follows:

1) Monitor flowing pressures and shut-in pressures of producing wells.
2) Use CBM material balance equation to match existing shut-in pressures.
3) Use radial flow equations (Eq. 1 for gas + radial flow equation for water) to solve for effective permeability to each phase as a function of the reservoir pressure calculated with calibrated material balance equation (step 2). Alternatively, once either k_g or k_w are known, the other can be calculated from the k_{rg}/k_{rw} ratio calculated using Eq. 27 (ignoring solution gas).
4) Estimate mobile water saturation as a function of cumulative water production:
   a. Estimate initial mobile water volume-in-place from rate-time analysis of produced water. This assumes that water production is recorded accurately.
   b. Calculate mobile water saturation as a function of cumulative water production (STB) using material balance equation for water. The simplest water material balance equation that can be used (assuming a volumetric reservoir) is:

$$S_w = S_{wi} - \frac{Q_w}{N_w} \qquad \text{(A-1)}$$

The denominator of the second term on the right hand side of the Eq. A-1 equation is the initial mobile water – in-place (STB), calculated from step 4a. The first term on the right hand side is the initial mobile water saturation.

5) Plot effective permeability to gas and water as a function of mobile water saturation.
6) Estimate base permeability – the best time to estimate an absolute permeability is when the reservoir is in single-phase flow, either dominated by gas or water flow. For example, in undersaturated coal reservoirs, early time water production data (prior to onset of significant gas production) may be used to estimate absolute permeability (effective permeability to water). In the San Juan Basin Fruitland Coal Fairway, the coals are saturated, and two-phase production occurs immediately. For these coals, the effective permeability to gas at a reservoir pressure corresponding to negligible relative permeability to gas growth (S_w changing slowly after dewatering phase), was used as a base permeability. It should be noted that at reservoir pressures greater than the selected base permeability, it is anticipated that some base permeability changes are incorporated into the relative permeability curves.
7) Divide effective permeabilities to gas and water by base permeability to generate relative permeability curves as function of water saturation.

Appendix B

The Harpalani and Pariti[34] and Extended Langmuir[19] approaches for modeling free-gas compositions (in equilibrium with a mixed adsorbed gas) both require the same input: single component Langmuir isotherm parameters, an accurate estimation of reservoir pressure and an initial free gas composition, at the start of the model projections. The single component Langmuir adsorption isotherm for gas is well known, and is re-stated below:

$$V = \frac{V_L bp}{1+bp} \quad \text{……(B-1)}$$

Where V_L and b are the Langmuir isotherm parameters obtained from fitting Eq. B-1 to experimental adsorption isotherm data for single-component gases such as methane and carbon dioxide. For field applications, it is assumed that the Langmuir parameters have been corrected to in-situ conditions[19].

Harpalani and Pariti Method[34]. This method for calculating free-gas compositions in equilibrium with a binary adsorbed gas mixture assumes that each adsorbed gas occupies a fixed fraction of the coal surface. The fraction may be adjusted along with single-component adsorption isotherm parameters to achieve a match of produced gas compositions during depletion. The procedure for a binary gas mixture of methane and carbon dioxide, a version of which was originally described by Harpalani and Pariti[34], is as follows:

1) Obtain the single component isotherm parameters (V_L and b) for both gaseous components from fit to experimental data and correct to in-situ conditions.
2) Plot the adsorbed gas amount for each component versus pressure (set initial pressure equal to initial reservoir pressure) for each component using the Langmuir equation and the obtained isotherm parameters from step 1).
3) Multiply the amount of methane adsorbed at each pressure step by a fraction, f (and 1-f, for carbon dioxide). These isotherms are referred to as the "adjusted" isotherms. The adjusted isotherms for each component may be summed to calculate a total numerical (composite) isotherm.
4) Calculate the desorption of methane at each pressure step by subtracting the amount of methane calculated with the adjusted isotherm from the lower pressure step from the preceding higher pressure step. Perform the same procedure for carbon dioxide. The sum of the desorbed amounts of methane and carbon dioxide at a pressure step, calculated from the adjusted isotherm, is the total gas desorbed at that pressure step.
5) The percentage of each component at each pressure step is determined by dividing the amount desorbed at each pressure step (see step 4) by the total desorbed gas amount, calculated from the adjusted isotherms.
6) Compare the percentages of each component calculated in step 5 with the produced gas compositions over the appropriate pressure range. If there is no match, then f may be adjusted, and steps 3 – 6 repeated until a match is obtained. In some cases, the pure component isotherm parameters may also require adjustment, in which case steps 1 – 6 are repeated until a match is obtained.

Once the "match" to the produced gas compositions is achieved, the composite (mixed gas) isotherm parameters may be obtained by fitting Eq. B-1 to the total numerical (composite) isotherm obtained during step 3. This composite isotherm is to be used in material balance calculations, as described in the text.

Extended Langmuir Method. The Extended Langmuir equation, given below, has been used extensively for modeling binary and multi-component gas adsorption on coal[19].

$$V_i = \frac{V_{Li} b_i p y_i}{1+\sum_j b_j p y_j} \quad \text{……(B-2)}$$

Where V_i is the amount of component "i" adsorbed, V_{Li} and b_i are constants in the Langmuir equation for component "i", and y_i is the mole fraction of component "i" in the free-gas phase (in equilibrium with adsorbed gas). The total amount adsorbed is simply:

$$V_T = \sum_i \left(\frac{V_{Li} b_i p y_i}{1+\sum_j b_j p y_j} \right) \quad \text{……...……..…(B-3)}$$

The adsorbed phase mole fractions of each component in a binary system may be obtained by noting:

$$\frac{V_1}{V_2}=\frac{x_1}{x_2}=\frac{V_{L1}b_1y_1}{V_{L2}b_2y_2} \quad \text{.....(B-4)}$$

or:

$$\frac{x_1}{1-x_1}=\frac{x_1}{x_2}=\frac{V_{L1}b_1}{V_{L2}b_2}\frac{y_1}{1-y_1} \quad \text{.....(B-5)}$$

The gas-phase compositions in a binary gas system may be obtained using the following procedure, assuming tank-type depletion:

1) Obtain the single component isotherm parameters (V_L and b) for both gaseous components from fit to experimental data and correct to in-situ conditions.
2) Set the initial pressure and the initial free gas composition, y_{io}, then use Eq. B-5 to calculate the initial adsorbed-gas composition, x_{io}.
3) Use Eq. B-3 to calculate the total amount adsorbed, V_T, and Eq. B-2 to calculate the initial adsorbed amounts for each component (V_{1o} and V_{2o}).
4) Assume a step size for desorption: $\Delta V = C \times V_0$, where C is the amount of gas removed in each calculation step.
5) Calculate $\Delta V_i = C \times y_{io}$.
6) Calculate the amount of fluid remaining in tank after 1st depletion step: $V_i = V_{io} - \Delta V_i$.
7) Calculate adsorbed phase composition after 1st depletion step: $x_i = V_i / \left(V_i + V_j\right)$.
8) Calculate gas phase composition after 1st depletion step using Eq. B-5.
9) Calculate the pressure after 1st depletion step from Eq. B-2 or B-3.
10) Repeat steps 5 – 9 for each sequential desorption step until abandonment pressure is reached.

Appendix C

The following describes the various forms of the diffusivity equation that can be used for CBM reservoirs (assuming negligible desorption time) and the corresponding forms of the flowing material balance equation resulting from the solution to the diffusivity equation for boundary-dominated flow.

Single-Phase (water) CBM Reservoirs. Undersaturated CBM reservoirs may produce substantial volumes of water and negligible gas during the first few months of their producing life. If relative permeability effects are negligible and the well reaches boundary dominated flow during the undersaturated flow period, the FMB may be used to establish fluid-in-place and possibly permeability, analogous to its application for undersaturated oil reservoirs. Starting with the diffusivity equation for radial, single-phase flow of a slightly compressible fluid in a conventional single-porosity porous medium[42]:

$$\frac{1}{r}\frac{\partial}{\partial r}\left(r\frac{\partial p}{\partial r}\right)=\frac{\phi\mu_w c_t}{k}\frac{\partial p}{\partial t} \quad \text{.....(C-1)}$$

Where $c_t = c_w + c_f$, is the sum of the formation and fluid (water) compressibilities and ϕ is the fracture porosity (assuming water production only occurs from the fractures). The assumptions used in the derivation of this equation have been discussed elsewhere[42].

Following the work of Mattar and Anderson[10], the flowing material balance equation for a slightly compressible fluid (water in this case) may be derived from the solution to Eq. C-1, during pseudosteady-state flow, for a well centered in a closed, cylindrical reservoir, producing at a constant rate:

$$p_i - p_{wf} = \Delta p = \frac{q_w t}{c_t N_w} + \frac{141.2 B_w \mu_w q_w}{kh}\left(\ln\frac{r_e}{r_{wa}} - \frac{3}{4}\right) \quad \text{...(C-2)}$$

This solution is valid only for constant rate, so to extend to variable operating conditions (rate/pressure), material balance pseudotime is substituted for real time in Eq. C-2 as follows:

$$\Delta p = \frac{q_w t_c}{c_t N_w} + \frac{141.2 B_w \mu_w q_w}{kh}\left(\ln\frac{r_e}{r_{wa}} - \frac{3}{4}\right) \quad \text{.....(C-3)}$$

where:

$$t_c = \frac{Q_w}{q_w} \quad \text{.....(C-4)}$$

Re-arranging and setting $b_{pss} = \frac{141.2 B_w \mu_w}{kh}\left(\ln\frac{r_e}{r_{wa}} - \frac{3}{4}\right)$:

$$\frac{q_w}{\Delta p} = -\frac{Q_w}{\Delta p c_t}\frac{1}{N_w b_{pss}} + \frac{1}{b_{pss}} \quad \text{.....(C-5)}$$

Eq. C-5 is the flowing material balance equation for a slightly-compressible fluid flowing to a well centered in a cylindrical reservoir. In the case of an undersaturated CBM reservoir, the slightly compressible fluid is water, if there is negligible gas saturation. A plot of the left hand side vs. $Q/(\Delta p c_t)$ should be linear during the undersaturated, boundary-dominated flow period, and can be extrapolated to obtain fluid-in-place (N_w). If net pay of the reservoir is known, drainage area may be calculated. If skin is known, or can be reasonable approximated, the y-intercept may be used to estimate permeability from the b_{pss} term.

Single-phase (gas) CBM Reservoirs. The radial diffusivity equation for single-phase CBM reservoirs, with negligible desorption times, may be written as follows[43]:

$$\frac{1}{r}\frac{\partial}{\partial r}\left(\frac{p}{\mu_g z} r \frac{\partial p}{\partial r}\right) = \frac{\phi c_t}{k}\frac{p}{Z}\frac{\partial p}{\partial t} \quad \text{(C-6)}$$

where:

$$c_t = c_g + c_f + c_d \quad \text{(C-7)}$$

c_t is the sum of the gas, formation and desorption compressibility, which is in turn be defined as:

$$c_d = \frac{B_g \rho_c V_L p_L}{32.0368(p_L + p_R)^2 \phi} \quad \text{(C-8)}$$

Eq. C-6 assumes: radial/laminar flow in a porous medium with constant permeability and compressibility; negligible gravity effects; isothermal conditions; fluid obeys real-gas law; adsorption follows a Langmuir isotherm, and adsorption is instantaneous (no diffusion/sorption times are negligible). Eq. C-6 may be written in terms of pseudopressure as follows:

$$\frac{1}{r}\frac{\partial}{\partial r}\left(r\frac{\partial m(p)}{\partial r}\right) = \frac{\phi \mu_g c_t}{k}\frac{\partial m(p)}{\partial t} \quad \text{(C-9)}$$

where:

$$m(p) = 2\int_{p_b}^{p} \frac{p}{\mu_g Z} dp \quad \text{(C-10)}$$

As with conventional reservoirs, pseudotime may be introduced into the diffusivity equation to account for gas property variation with pressure[4] and to allow solutions for slightly compressible fluids to be used:

$$\frac{1}{r}\frac{\partial}{\partial r}\left(r\frac{\partial m(p)}{\partial r}\right) = \frac{\phi(\mu_g c_t)_i}{k}\frac{\partial m(p)}{\partial t_a} \quad \text{(C-11)}$$

where:

$$t_a = (\mu_g c_t)_i \int_0^t \frac{dt}{\overline{\mu}_g \overline{c}_t} \quad \text{(B-12)}$$

For CBM reservoirs (with instantaneous desorption), c_t must include desorption compressibility. Note that $\overline{\mu}_g \overline{c}_t$ is evaluated at the average reservoir pressure.

To obtain the FMB equation, we must first start with the (approximate) solution to Eq. C-11, assuming pseudo-steady state flow of gas for a well centered in a closed, cylindrical reservoir, producing at a constant rate:

$$m(p_i) - m(p_{wf}) = \Delta m(p) = \frac{2q_g p_i}{(\mu_g c_t Z)_i G_i} t_a + \frac{1.417x10^6 T q_g}{kh}\left(\ln\frac{r_e}{r_{wa}} - \frac{3}{4}\right) \quad \text{(C-13)}$$

Introducing material balance pseudodtime[7] to account for changing backpressure during boundary dominated flow, and re-arranging we arrive at the FMB equation for single-phase CBM reservoirs:

$$\frac{q_g}{[m(p_i) - m(p_{wf})]} = \frac{-2q_g t_{ca} p_i}{[m(p_i) - m(p_{wf})] * [\mu_g c_t Z]_i}\frac{1}{G_i b'_{pss}} + \frac{1}{b'_{pss}} \quad \text{(C-14)}$$

where:

$$t_{ca} = \frac{(\mu_g c_t)_i}{q_g}\int_0^t \frac{q_g dt}{\overline{\mu}_g \overline{c}_t} = \frac{(\mu_g c_t Z)_i}{q_g}\frac{G_i}{2P_i}[m(p_i) - m(p_R)] \quad \text{(C-15)}$$

and

$$b'_{pss} = \frac{1.417x10^6 T}{kh}\left(\ln\frac{r_e}{r_{wa}} - \frac{3}{4}\right) \quad \text{(C-16)}$$

The FMB may be written in the form of a straight line as given with Eq. 21, and used to estimate G_i and permeability (if skin can be estimated). In order to apply Eq. 21 for CBM reservoirs, $m(p_R)$ must be obtained using material balance equations that incorporate desorption effects and G_i must be calculated using the GIP equation for CBM reservoirs:

$$G_i = Ah\left(\frac{43560\phi(1 - S_{wi})}{B_{gi}} + 1.3597\rho_c V_i\right) \quad \text{(C-17)}$$

Two-Phase (gas+water) CBM Reservoirs. A radial diffusivity equation describing multiphase flow has been developed previously[42]:

$$\frac{1}{r}\frac{\partial}{\partial r}\left(r\frac{\partial p}{\partial r}\right) = \frac{\phi c_t}{\lambda_t}\frac{\partial p}{\partial t} \quad \text{(C-18)}$$

This equation looks much like the diffusivity equation for single-phase flow (Eq. C-1). In addition to the assumptions used to derive Eq. C-6., Eq. C-18 assumes that: effective permeability is a function of saturation, not pressure; saturation and pressure gradients are small, and there are negligible capillary effects. For CBM reservoirs (again assuming desorption is instantaneous), c_t and λ_t would be defined as follows[40]:

$$c_t = S_w c_w + S_g c_g + c_f + c_d \quad \text{(C-19)}$$

which accounts for gas, water, fracture pore volume and desorption compressibility,

and:

$$\lambda_t = \frac{k_g}{\mu_g} + \frac{k_w}{\mu_w} \quad \text{.....(C-20)}$$

King and Ertekin[43] presented a form of the diffusivity equation representing two-phase flow, written in terms of pseudopressure (a modification of the Kamal and Six[44] definition) and pseudotime (again ignoring desorption time):

$$\nabla^2 m^*(p) = \frac{\phi(\mu_g c_{eff})_i}{\alpha k_i} \frac{\partial m^*(p)}{\partial t_p} \quad \text{.....(C-21)}$$

where:

$$m^*(p) = 2\int_{p_b}^{p} k\left(\frac{\rho_g k_{rg}}{\rho_{wsc}\mu_g} + \frac{k_{rw}}{\mu_w B_w}\right) dp' \quad \text{.....(C-22)}$$

$$c_{eff} = \left[\frac{S_w}{B_w} + \frac{(1-S_w)\rho_g}{\rho_{wsc}}\right] c_f + \frac{S_w c_w}{B_w} + \frac{(1-S_w)\rho_g c_g}{\rho_{wsc}} + \frac{M_g}{\phi\rho_{wsc}} \frac{dC_E}{dp} \quad \text{..(C-23)}$$

$$t_p = \frac{(c_{eff}\mu_g)_i}{k_i} \int_{t_o}^{t} \frac{k\left(\frac{\rho_g k_{rg}}{\rho_{wsc}\mu_g} + \frac{k_{rw}}{\mu_w B_w}\right)}{c_{eff}} dt' \quad \text{.....(C-24)}$$

In radial coordinates, Eq. B-21 becomes:

$$\frac{1}{r}\frac{\partial}{\partial r}\left(r\frac{\partial m^*(p)}{\partial r}\right) = \frac{\phi(\mu_g c_{eff})_i}{\alpha k_i} \frac{\partial m^*(p)}{\partial t_p} \quad \text{.....(C-25)}$$

King and Ertekin[43] discuss in detail how to calculate the pseudopressure function (Eq. C-22); the reader is referred to that work for a discussion of appropriate algorithms. At present, we have not used this equation to derive a multiphase FMB for coal.

For CBM reservoirs where gas flow dominates (ex. as with some saturated CBM reservoirs after significant dewatering), Eq. C-6 may be modified to include the saturation-dependence of k_g:

$$\frac{1}{r}\frac{\partial}{\partial r}\left(\frac{p}{\mu_g Z} r \frac{\partial p}{\partial r}\right) = \frac{\phi c_t}{k_g(S_g)} \frac{p}{Z} \frac{\partial p}{\partial t} \quad \text{.....(C-26)}$$

In addition to the assumptions used in the derivation of Eq. C-6, Eq. C-26 assumes that k_g is dependent upon a single saturation value (S_g = 1- S_w) within the domain of the reservoir (i.e. drainage volume of a well), that varies during pressure depletion. The solution to this equation therefore requires an independent estimate of water saturation changes during depletion (corresponding to the pore-volume average pressure at each time-step). Mavor[40] presented a CBM well-test analysis approach for CBM wells dominated by gas production and successfully applied it to a Warrior Basin CBM well. Eq. C-26 can be written in terms of gas-phase pseudopressure as follows:

$$\frac{1}{r}\frac{\partial}{\partial r}\left(r\frac{\partial m(p)}{\partial r}\right) = \frac{\phi\mu_g c_t}{k_g(S_g)} \frac{\partial m(p)}{\partial t} \quad \text{.....(C-27)}$$

Again, pseudotime may be introduced into Eq. C-27 to account for gas property variation with pressure. The FMB equation can be derived for this simplified equation in a similar way to the single-phase gas CBM case, resulting in:

$$\frac{q_g}{[m(p_i) - m(p_{wf})]k_{rg}(S_g)} = \frac{-2q_g t_{ca} p_i}{[m(p_i) - m(p_{wf})] * [\mu_g c_t Z]_i} \frac{1}{G_i b'_{pss}} + \frac{1}{b'_{pss}} \quad \text{....(C-28)}$$

where b'_{pss} is the same as Eq. C-16 and G_i and k can be obtained in a similar way to the single-phase gas case described above.

Relative permeability to gas, which appears on the left hand side of Eq. C-28, is a function of gas saturation, which may be determined using gas and water production data, combined with relative permeability curve information, as described in the text, or from material balance (ex. King's method[31]). Eq. C-28, which accounts for relative permeability effects during depletion, does not account for relative permeability gradients in the reservoir cause by saturation gradients. An approximate method for accounting for saturation gradients is to include k_{rg} into the definition of pseudopressure as given below:

$$m^*(p) = 2\int_{p_b}^{p} \frac{p k_{rg}(p)}{\mu_g Z} dp \quad \text{.....(C-29)}$$

This approach requires that a relationship between k_{rg} and pressure be developed. In this work, we have correlated k_{rg} to the volumetric average pressure of the reservoir, as determined from simulation or material balance, for simplification. A more rigorous approach would be to develop this relationship for both p_{wf} and p_R and using those correlations in the calculation of $m^*(p_{wf})$ and $m^*(p_R)$, respectively. For the simple examples analyzed thus far, we have not found that this approach has improved the accuracy of OGIP or k calculations, but may be necessary in practice.

CBM Reservoirs with k_g Growth. For the case where effective permeability to gas growth occurs due to a combination of relative permeability and absolute permeability effects, the diffusivity equation looks similar to Eq. C-27, but with k_g assumed to be a function of pressure only:

$$\frac{1}{r}\frac{\partial}{\partial r}\left(r\frac{\partial m(p)}{\partial r}\right) = \frac{\phi\mu_g c_t}{k_g(p)} \frac{\partial m(p)}{\partial t} \quad \text{.....(C-30)}$$

As described in the text, the authors have found that the Fruitland Coal Fairway wells exhibit an exponential increase

in k_g as a function of volumetric average pressure for the reservoir. For these cases, the FMB may be written as:

$$\frac{q_g}{\left[m(p_i)-m(p_{wf})\right]k_g(p_R)} = \frac{-2q_g t_{ca} p_i}{\left[m(p_i)-m(p_{wf})\right]*\left[\mu_g c_t Z\right]_i}\frac{1}{G_i b^*_{pss}} + \frac{1}{b^*_{pss}} \quad ..(C\text{-}31)$$

where:

$$b^*_{pss} = \frac{1.417x10^6 T}{h}\left(\ln\frac{r_e}{r_{wa}} - 0.75\right) \quad .....(C\text{-}32)$$

If necessary, k_g may also be incorporated into the definition of pseudopressure to partially account for pressure/saturation gradients. Again, we have not found this to be necessary for the Fairway Coal wells analyzed to date.

Appendix D

Dimensionless variables used in the modified Fetkovich type-curves for single-phase coal analysis:

$$q_D = \frac{T}{0.000703kh\left[m(p_i)-m(p_{wf})\right]}q_g \quad .....(D\text{-}1)$$

$$q_{Dd} = q_D\left[\ln(r_e/r_{wa}) - 3/4\right] \quad .....(D\text{-}2)$$

$$t_D = \frac{0.00634k}{\left(\phi\mu_g c_t\right)_i r_{wa}^2}t_{ca} \quad .....(D\text{-}3)$$

$$t_{Dd} = \frac{2}{\left[(r_e/r_{wa})^2 - 1\right]\left[\ln(r_e/r_{wa}) - 3/4\right]}t_D \quad .....(D\text{-}4)$$

Eq. D-5: D-11 are used to extract permeability, skin, drainage area, pore-volume and bulk volume (at the onset of boundary-dominated flow), using the matches of production data to the Fetkovich type-curves:

$$k = \left(\frac{q}{q_{Dd}}\right)_{match}\left(\frac{T}{0.000703h\left[m(p_i)-m(p_{wf})\right]}\right)\left(\ln\left(\frac{r_e}{r_{wa}}\right)_{match} - \frac{3}{4}\right) \quad ... (D\text{-}5)$$

$$r_{wa}^2 = \left(\frac{t_{ca}}{t_{Dd}}\right)_{match}\frac{0.00634k}{\phi\mu_g c_t \frac{1}{2}\left(\left(\frac{r_e}{r_{wa}}\right)^2_{match} - 1\right)\left(\ln\left(\frac{r_e}{r_{wa}}\right)_{match} - \frac{3}{4}\right)} \quad ...(D\text{-}6)$$

$$s = \ln\left(\frac{r_w}{r_{wa}}\right) \quad .....(D\text{-}7)$$

$$r_e = r_{wa}\left(\frac{r_e}{r_{wa}}\right)_{match} \quad .....(D\text{-}8)$$

$$V_p = \left(\frac{t_{ca}}{t_{Dd}}\right)_{match}\left(\frac{q}{q_{Dd}}\right)_{match}\frac{2000\,p_{sc}T}{\left(\mu_g c_t\right)_i T_{sc}\left[m(p_i)-m(p_{wf})\right]} \quad ..(D\text{-}9)$$

$$V_b = \left(\frac{t_{ca}}{t_{Dd}}\right)_{match}\left(\frac{q}{q_{Dd}}\right)_{match}\frac{2000P_{sc}T}{\left(\phi\mu_g c_t\right)_i T_{sc}\left[m(p_i)-m(p_{wf})\right]} \quad (D\text{-}10)$$

Assuming a circular drainage area:

$$r_e = \sqrt{V_b/\pi h} \quad .....(D\text{-}11)$$

The analytical gas-in-place equation of Palacio and Blasingame[7] may be used to estimate GIP associated with fracture pore volume as follows:

$$G_i = \frac{2p_i}{\left(Z\mu c_t\right)_i}\left(\frac{t_{ca}}{t_{Dd}}\right)_{match}\left(\frac{q/\Delta m(p)}{q_{Dd}}\right)_{match} \quad .....(D\text{-}12)$$

TABLE 1. RESERVOIR DATA FOR HORSESHOE CANYON CBM WELL EXAMPLE.

INPUT PARAMETER	PARAMETER VALUE
THICKNESS (ft)	49.9
BULK DENSITY (g/cm^3)	1.33
CLEAT POROSITY (%)	0.1
GAS GRAVITY	0.55
INITIAL RESERVOIR PRESSURE (psia)	86
RESERVOIR TEMPERATURE (ºF)	67
LANGMUIR VOLUME (scf/ton, in-situ)	155
LANGMUIR PRESSURE (psia)	547

TABLE 2. RESERVOIR AND WELL PROPERTIES FOR SIMULATED UNDERSATURATED CBM EXAMPLE.

INPUT PARAMETER	PARAMETER VALUE
DRAINAGE AREA (acres)	80.0
THICKNESS (ft)	22.0
BULK DENSITY (g/cm^3)	1.37
CLEAT POROSITY (%)	0.7
GAS GRAVITY	0.62
INITIAL RESERVOIR PRESSURE (psia)	1270
RESERVOIR TEMPERATURE (ºF)	95
LANGMUIR VOLUME (scf/ton, in-situ)	409
LANGMUIR PRESSURE (psia)	743
% UNDERSATURATION (%)	30
PORE COMPRESSIBILITY ($psia^{-1}$)	4.0E-4
INITIAL WATER SATURATION (%)	100
RELATIVE PERMEABILITY	See Fig. 5a
WELLBORE RADIUS (ft)	0.25
PERMEABILITY (md)	5
SKIN	0
SORPTION TIME (days)	1.4

TABLE 3. RESERVOIR AND WELL PROPERTIES FOR SIMULATED TWO-PHASE EXAMPLE.

INPUT PARAMETER	PARAMETER VALUE
DRAINAGE AREA (acres)	80.0
THICKNESS (ft)	64.0
BULK DENSITY (g/cm^3)	1.33
CLEAT POROSITY (%)	13
GAS GRAVITY	0.554
INITIAL RESERVOIR PRESSURE (psia)	250
RESERVOIR TEMPERATURE (ºF)	65
LANGMUIR VOLUME (scf/ton, in-situ)	218.4
LANGMUIR PRESSURE (psia)	1355
% UNDERSATURATION (%)	0
PORE COMPRESSIBILITY ($psia^{-1}$)	1.0E-4
INITIAL WATER SATURATION (%)	95
RELATIVE PERMEABILITY	See Fig. 7a
WELLBORE RADIUS (ft)	0.5
PERMEABILITY (md)	100
SKIN	0
SORPTION TIME (days)	2

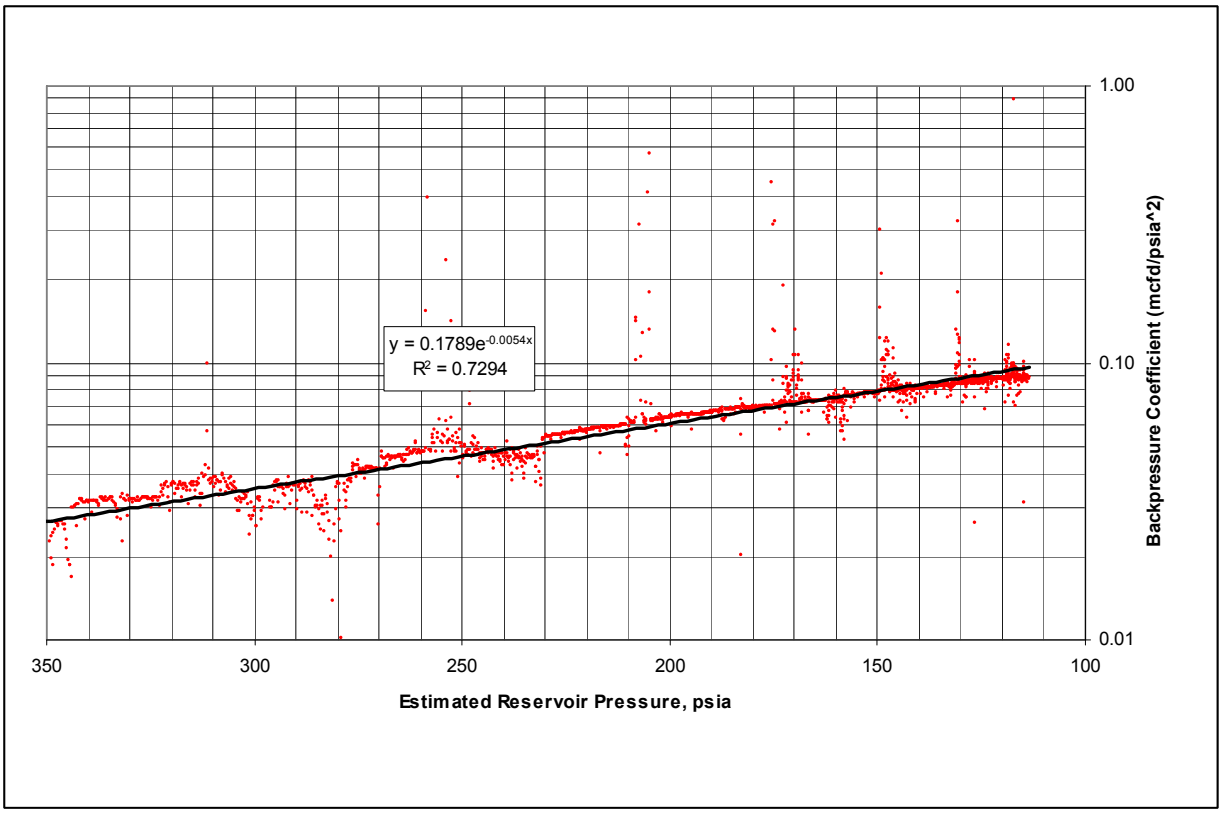

Fig. 1 — Example of trend in C coefficient (calculated using back-pressure equation) for Fairway Fruitland Coal well. The trend was interpreted to be exponential and due mainly to absolute permeability growth associated with matrix-shrinkage. Source: Gierhart *et al.*[24]

(a)

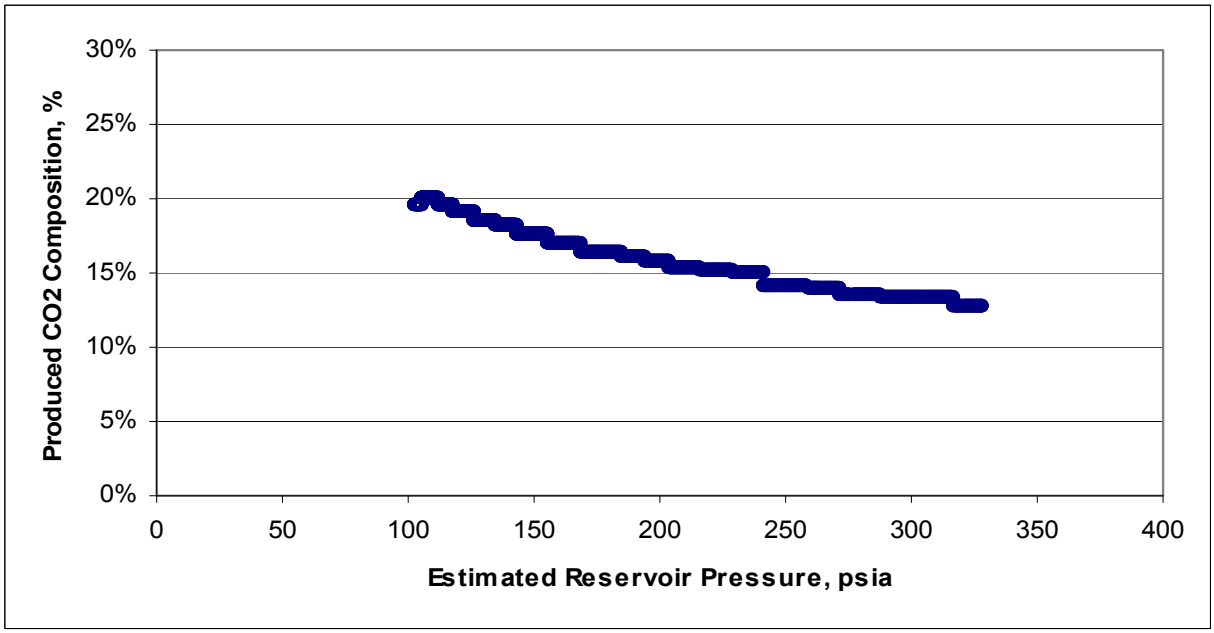

(b)

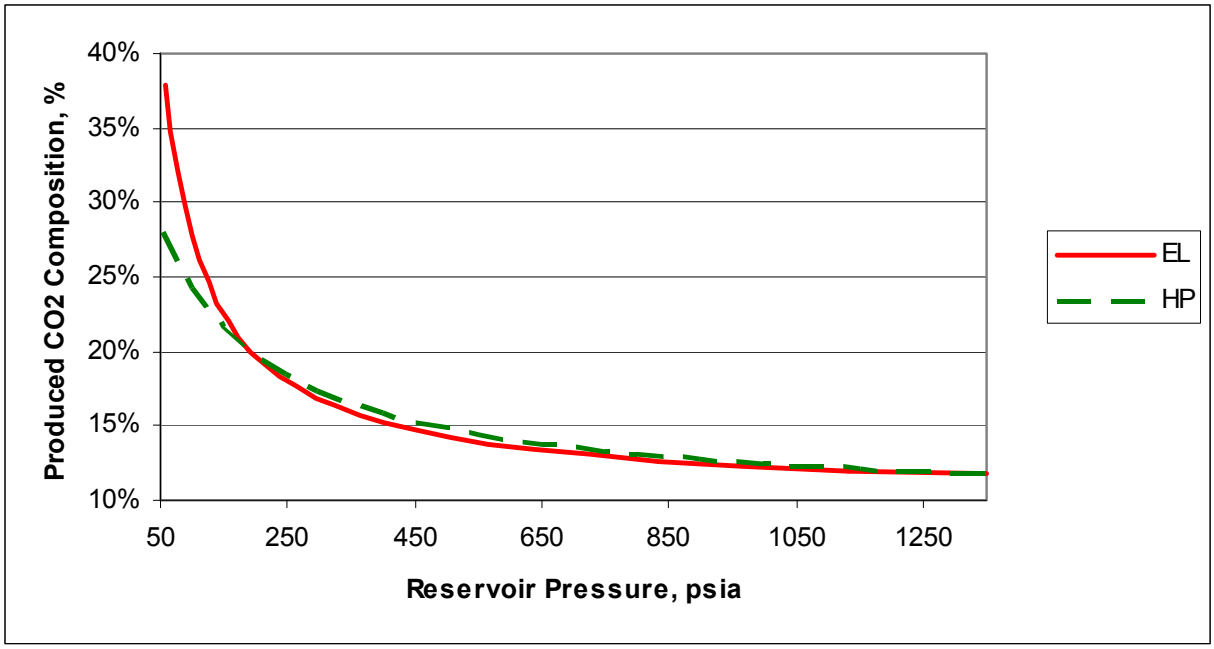

Fig. 2 — (a) Produced CO_2 composition (mole %) as a function of depletion for a Fairway Fruitland Coal CBM well ; (b) comparison of Harpalani-Pariti and Extended Langmuir model predictions given the same isotherm inputs.

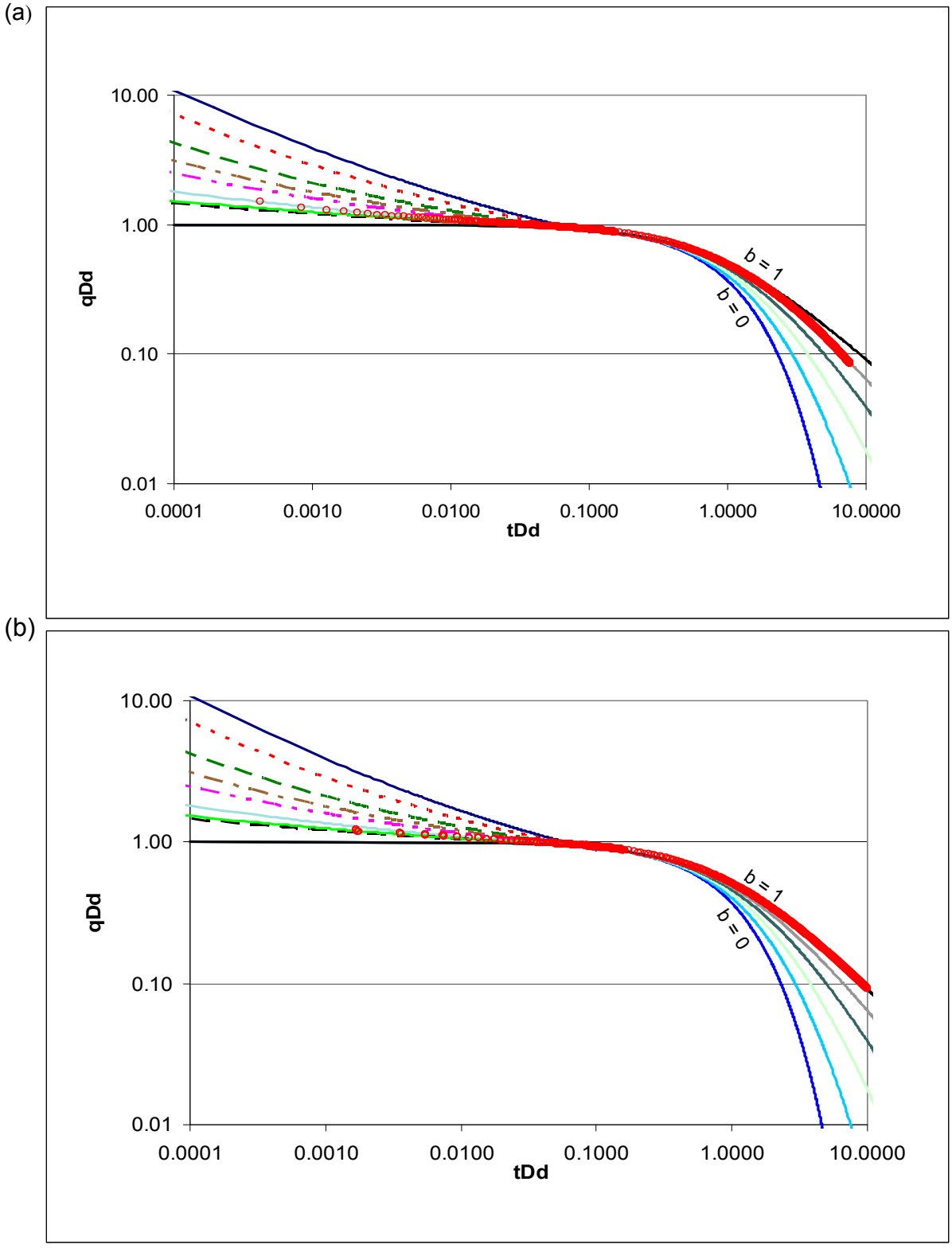

Fig. 3 — Fetkovich type-curve match of simulated single-phase CBM well production data. Type-curves generated using: (a) real time in dimensionless time function; (b) material balance pseudotime. Note that the use of material balance pseudotime forces the boundary-flow dominated production down the harmonic stem (b=1).

(a)

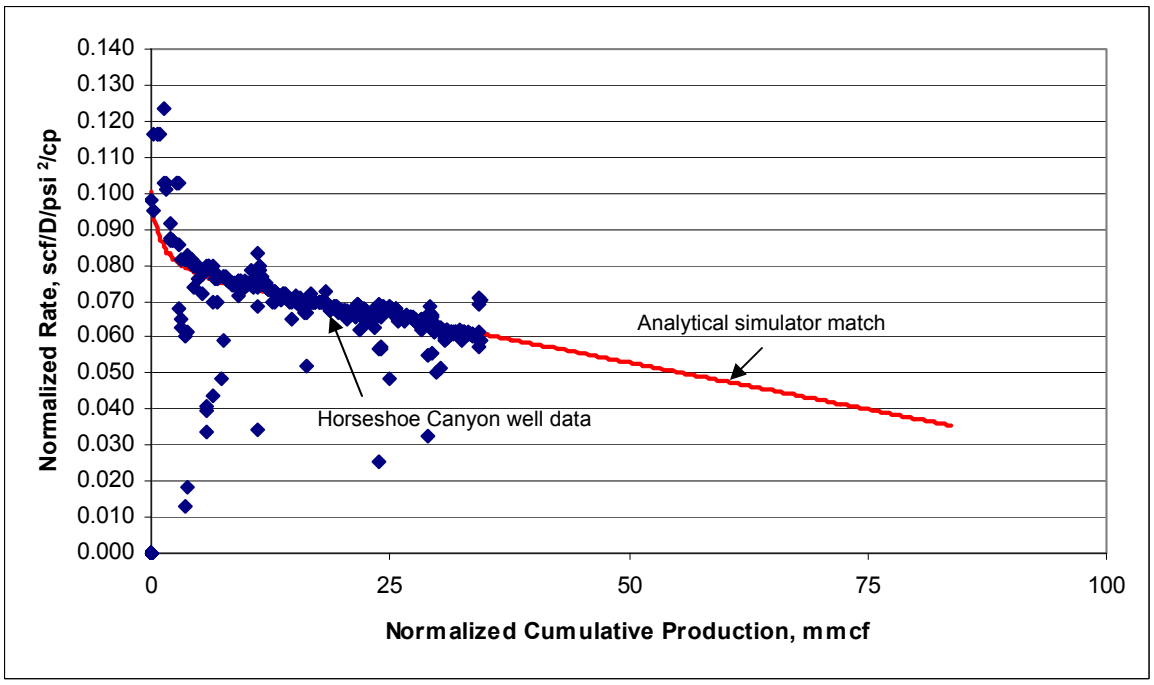

(b)

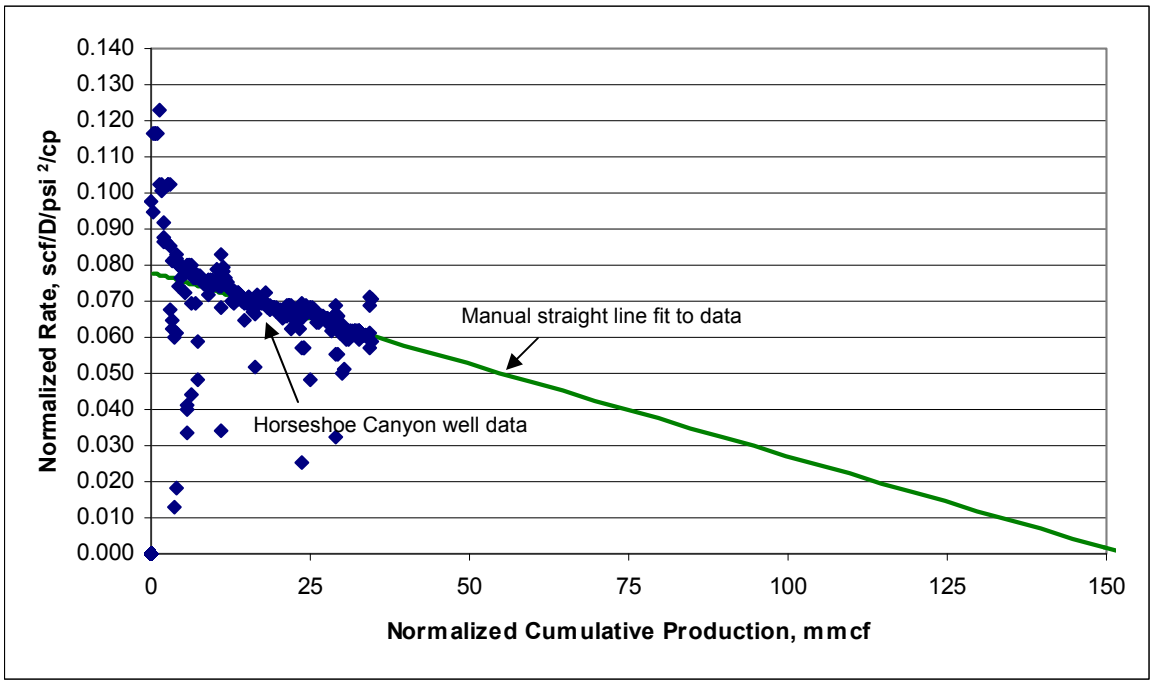

Fig. 4 — FMB plot of Horseshoe Canyon CBM well data: (a) analytical simulator match to data; b) straight line fit to data.

(a)

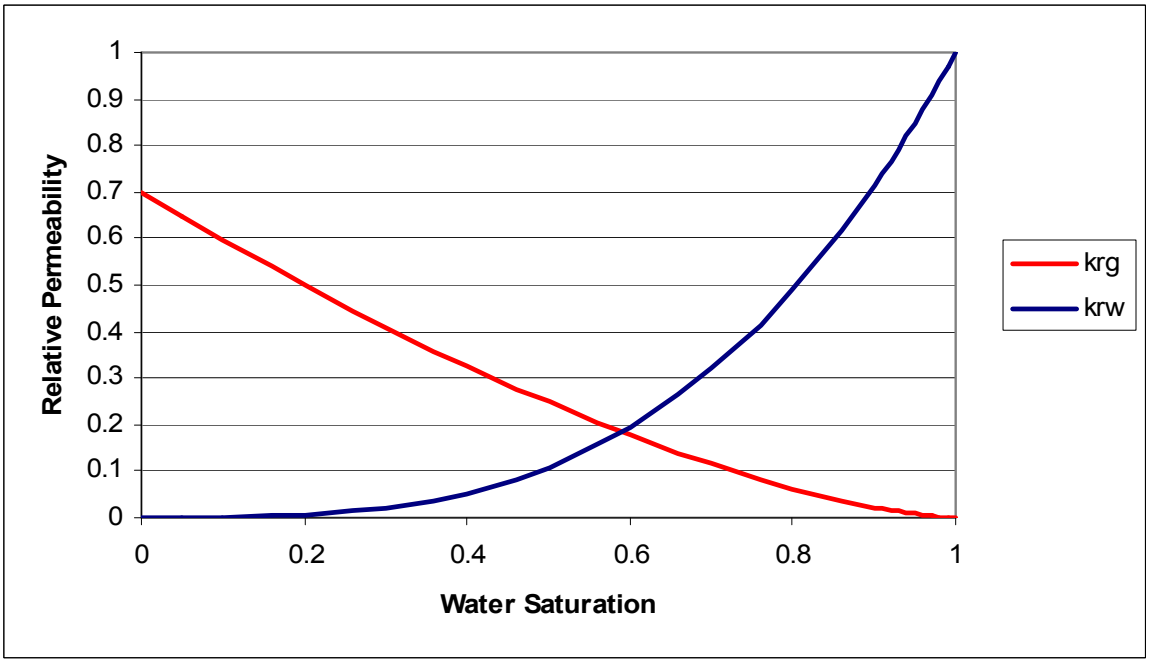

(b)

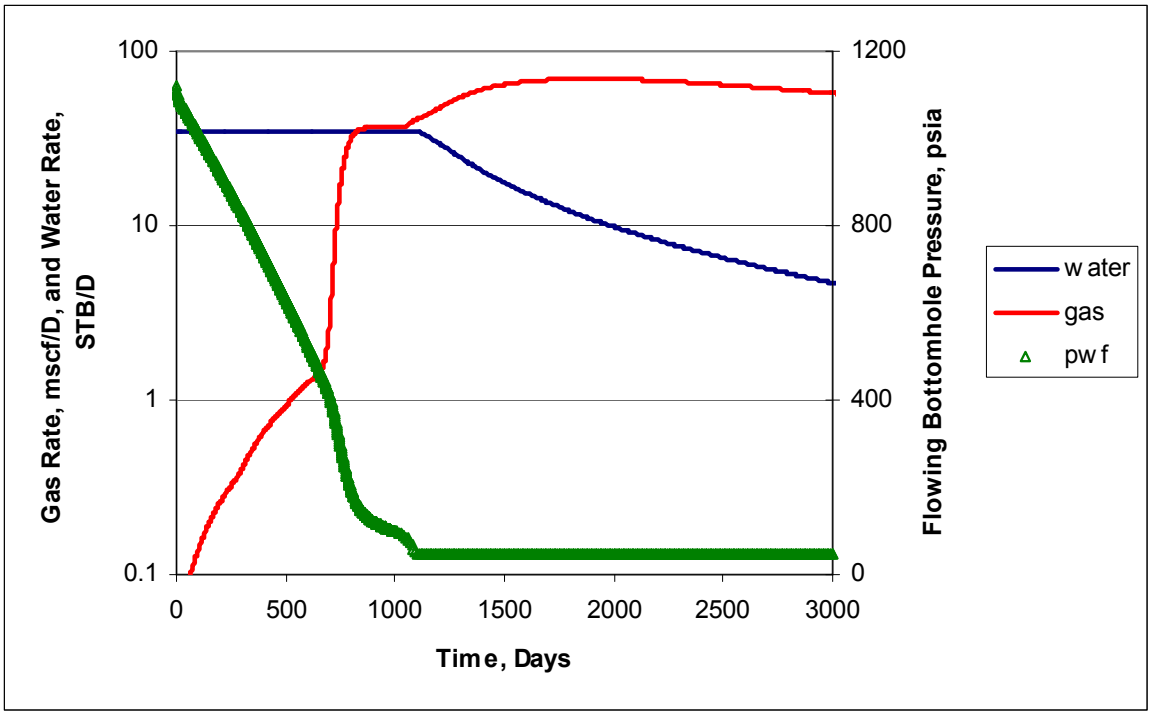

Fig. 5 — (a) Relative permeability curves used in simulated undersaturated CBM example; (b) simulated gas and water production and flowing bottomhole pressure profiles.

(a)

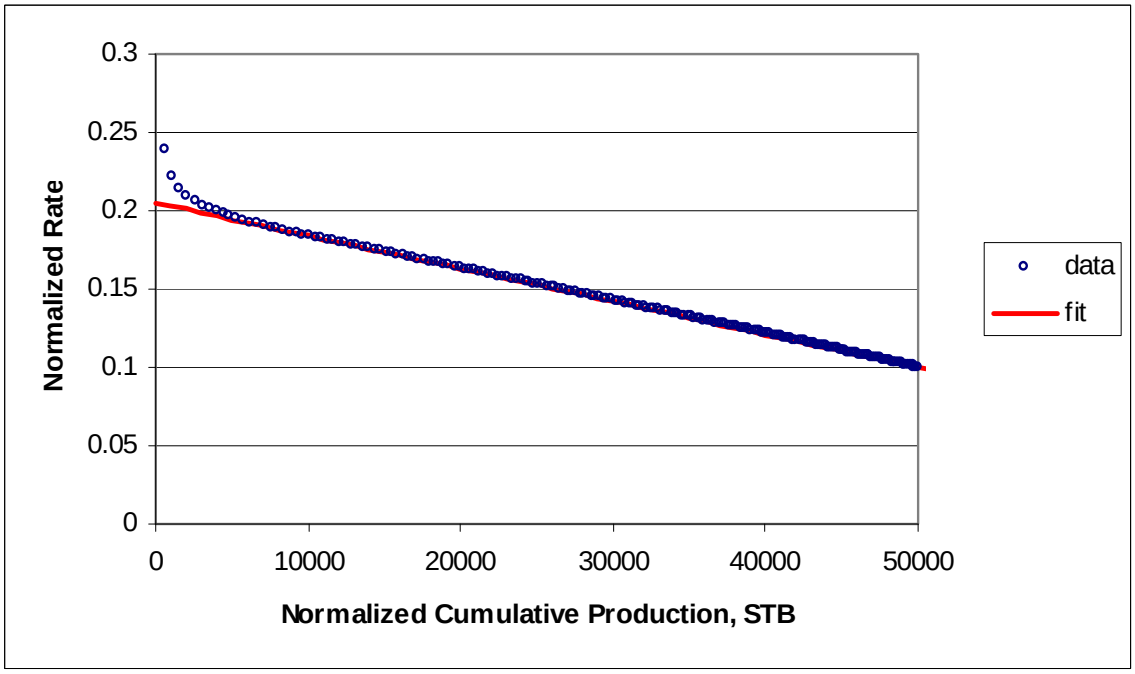

(b)

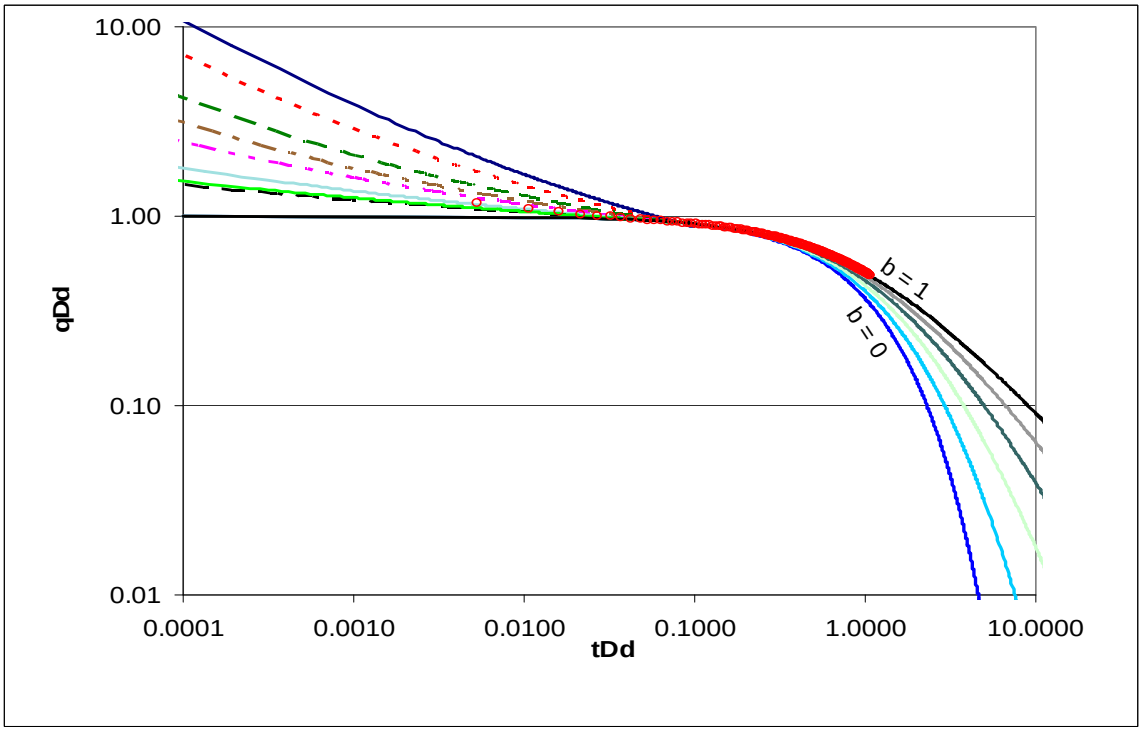

Fig. 6 —(a) FMB plot and (b) Fetkovich type-curve match of simulated water production for undersaturated CBM example. Only the first 200 days of production data were used.

(a)

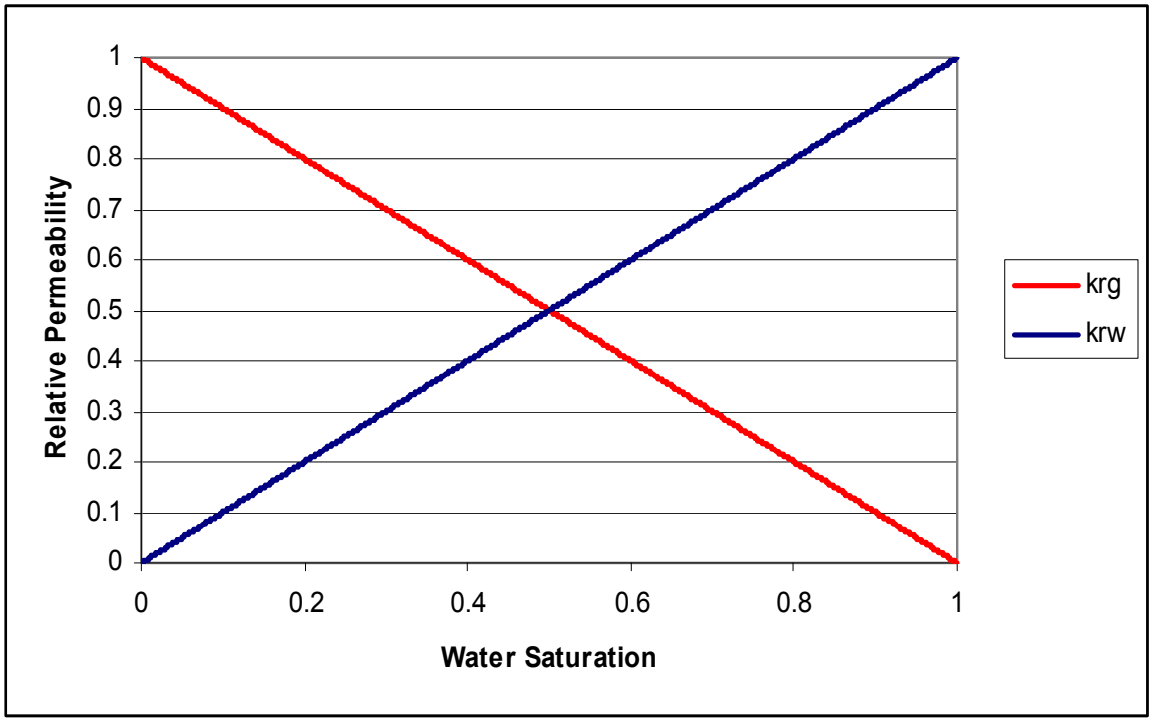

(b)

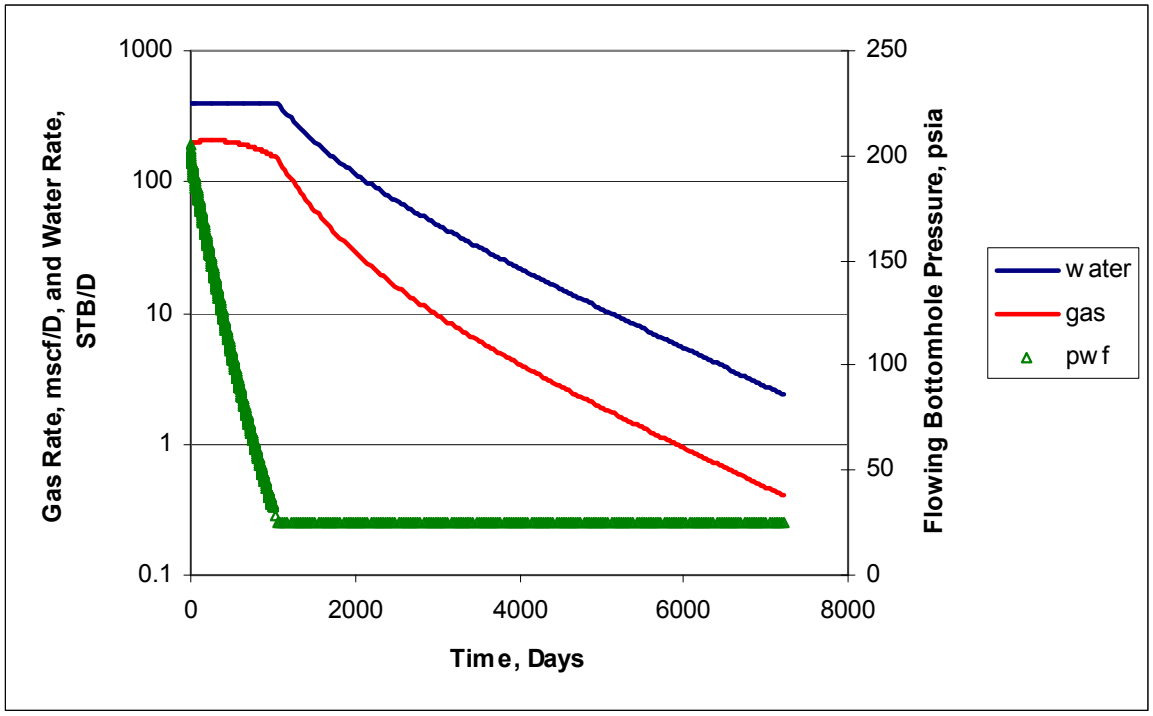

Fig. 7 — (a) Relative permeability curves used in simulated two-phase CBM example; (b) simulated gas and water production and flowing bottomhole pressure profiles.

(a)

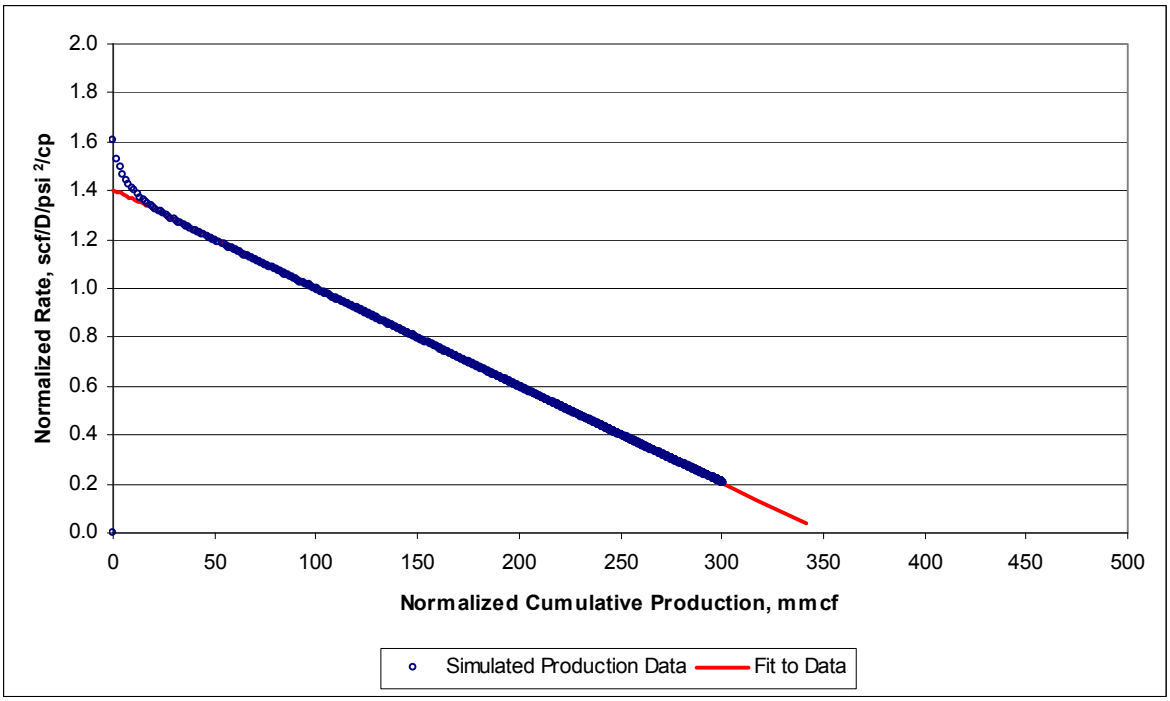

(b)

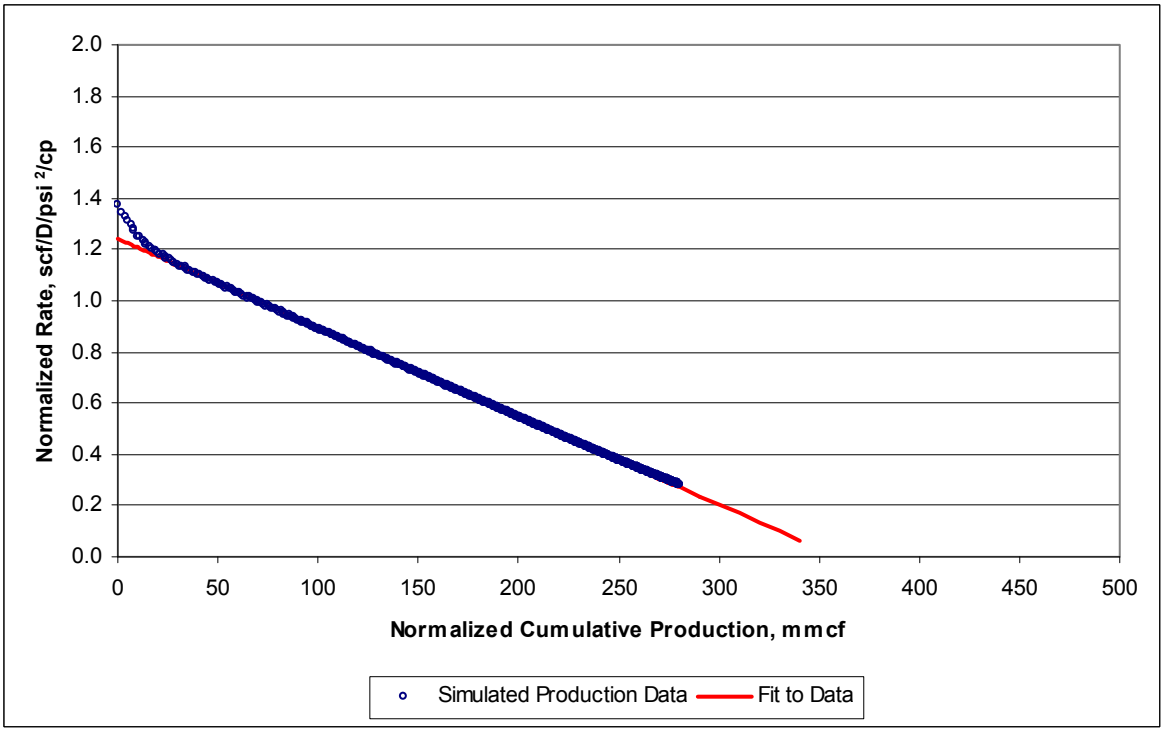

Fig. 8 — FMB plot of simulated gas production data for two-phase CBM example: (a) FMB without relative permeability included in pseudopressure calculation; b) FMB with relative permeability included in pseudopressure calculation. Straight line fit to data also shown.

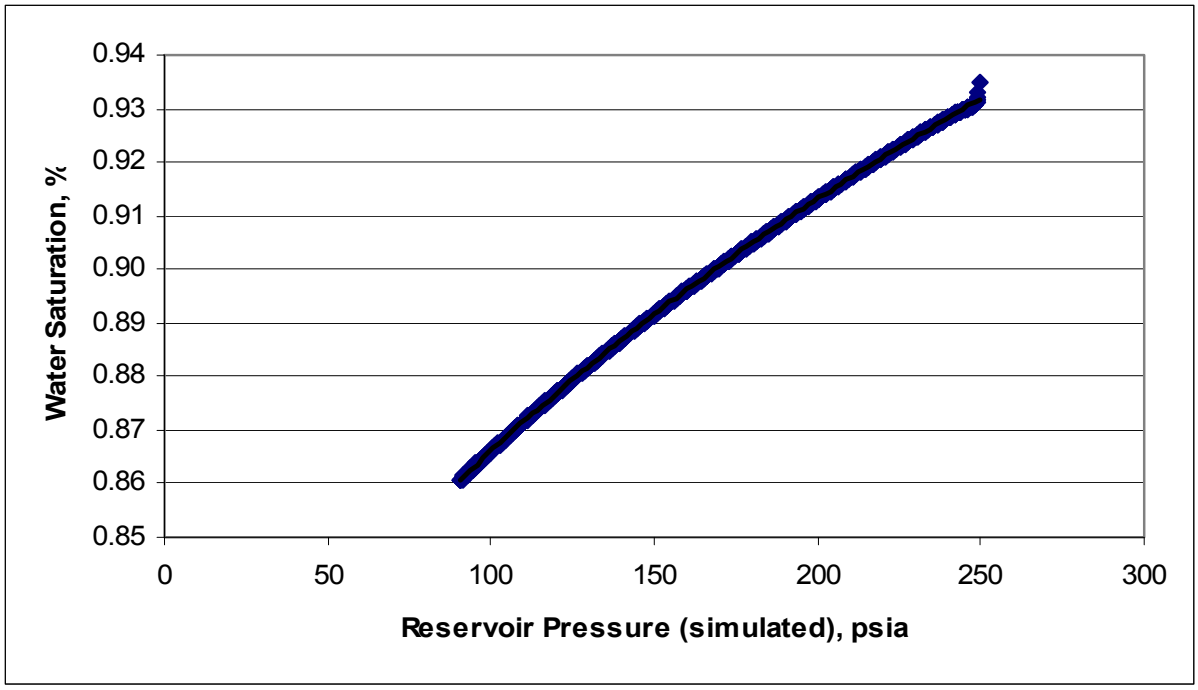

Fig. 9 — Relationship between water saturation and reservoir pressure used in pseudopressure calculations for two-phase CBM example.

(a)

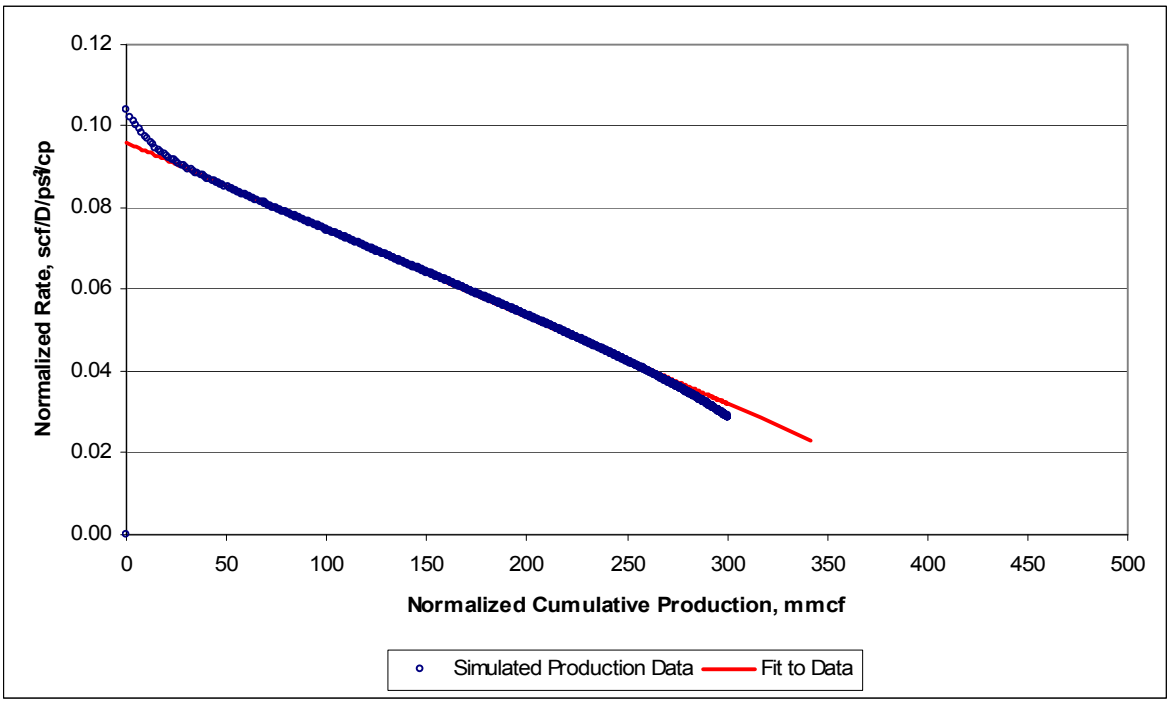

(b)

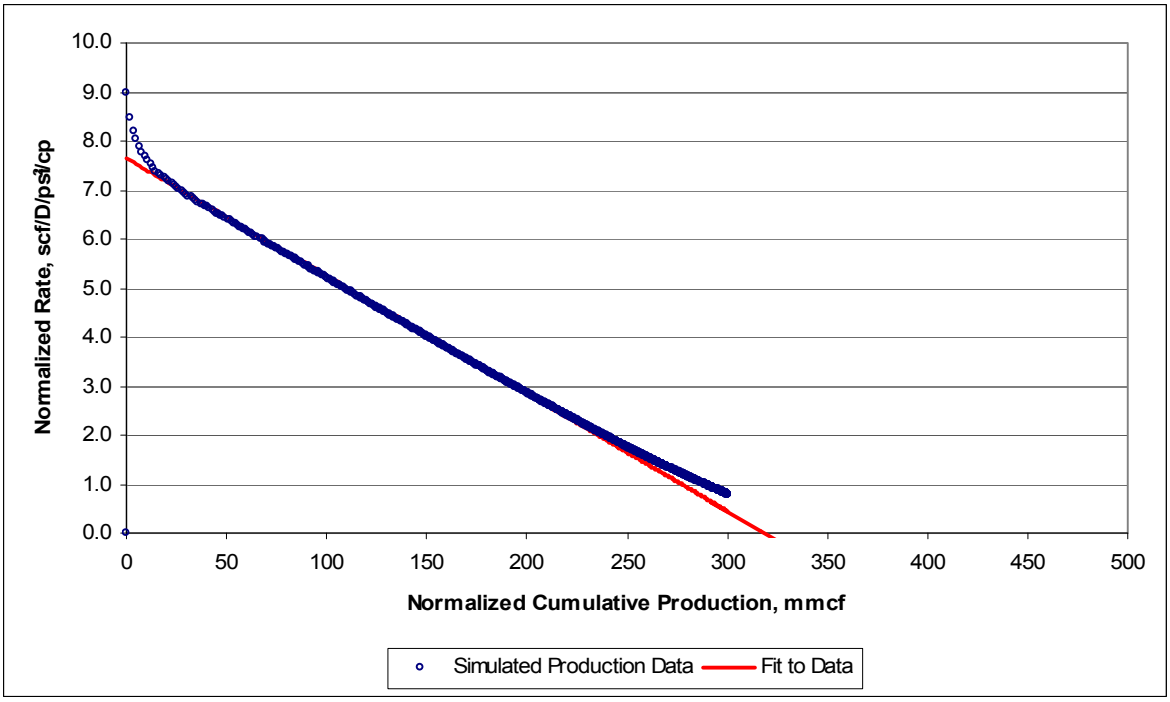

Fig. 10 — FMB plot of simulated gas production data for two-phase CBM example: (a) without relative permeability curve; b) with wrong relative permeability curve assumed. Straight line fit to data also shown. Compare results with Fig. 8a.

(a)

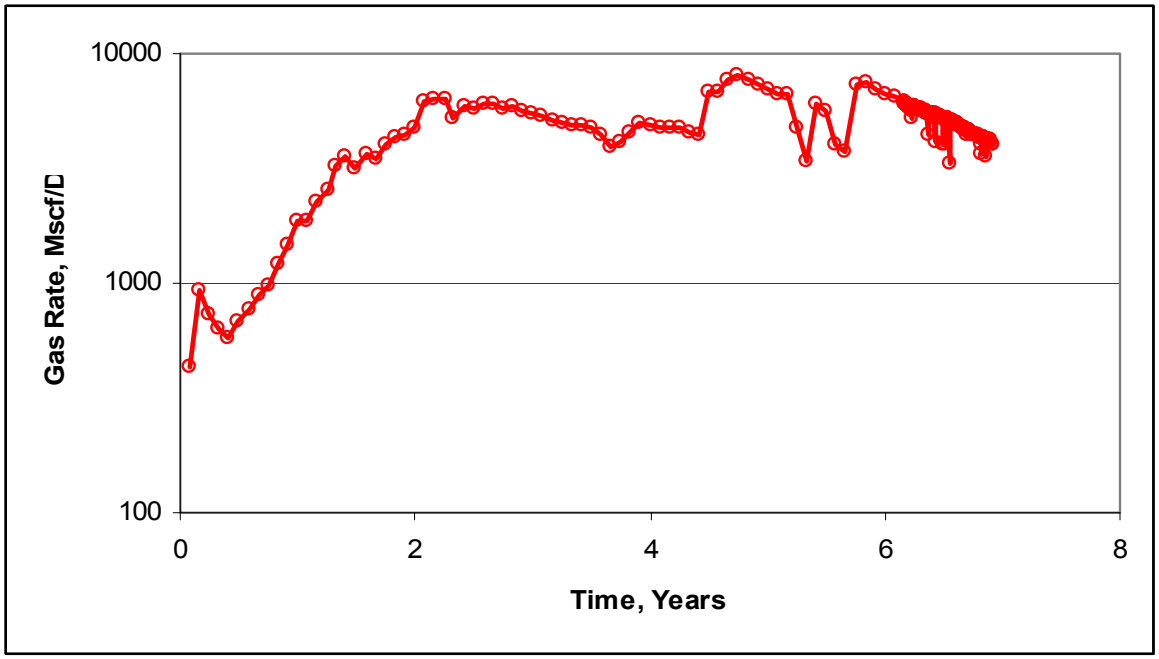

(b)

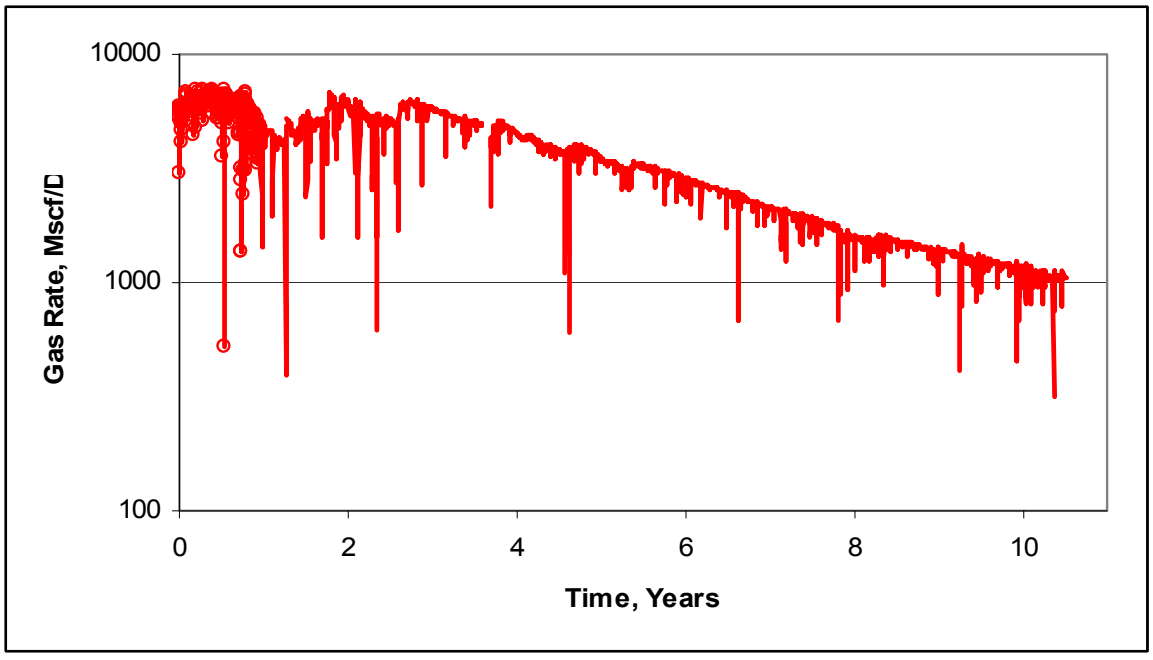

Fig. 11 — Fairway Fruitland Coal well gas production data used for analysis: (a) well 1 has mostly monthly production data ; (b) well 2 has daily data.

(a)

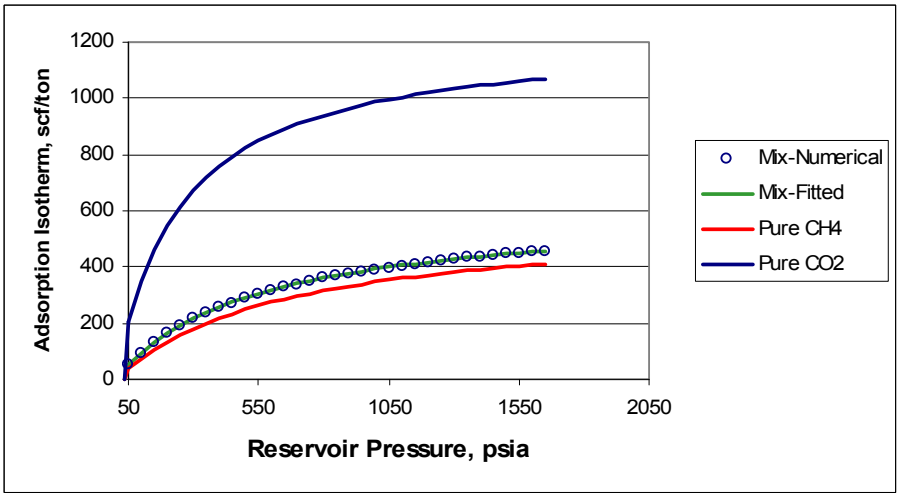

(b)

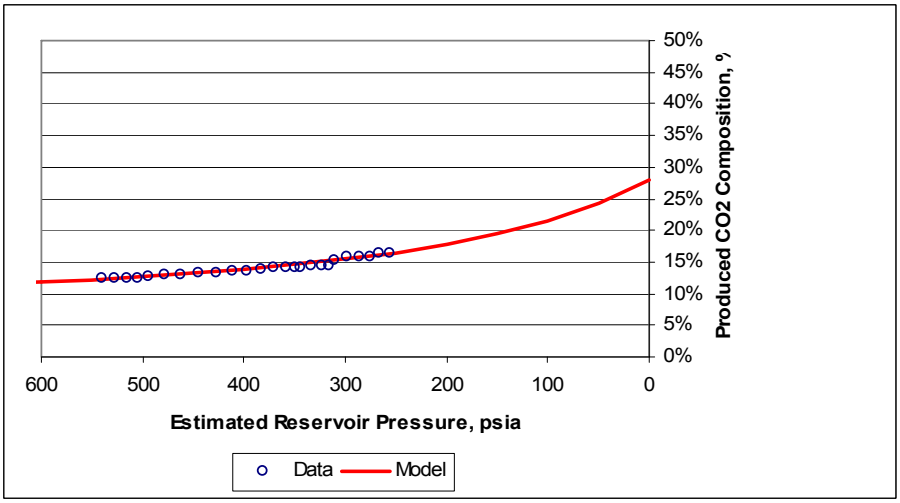

(c)

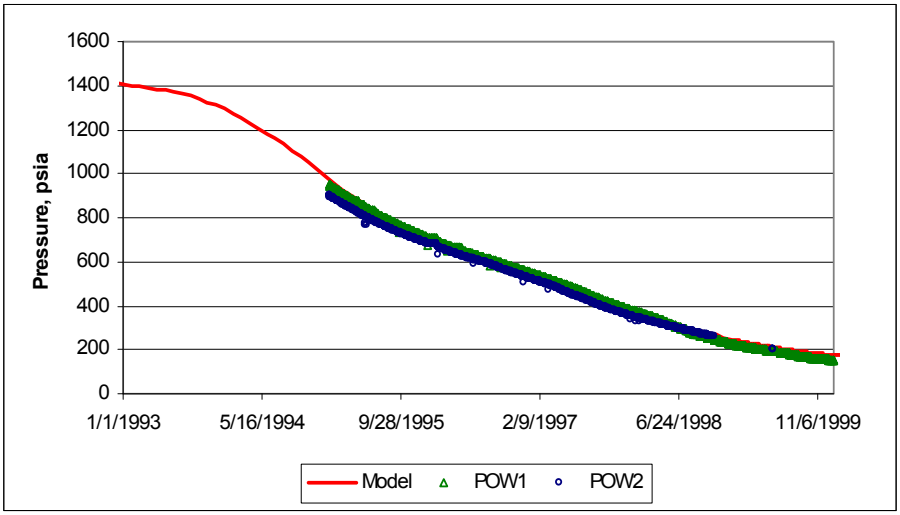

Fig. 12 — Well 1 modeling results : (a) individual and composite isotherms used to match produced gas compositions; (b) match of gas compositions with HP technique; (c) match to offset pressure observation well (POW) data.

(a)

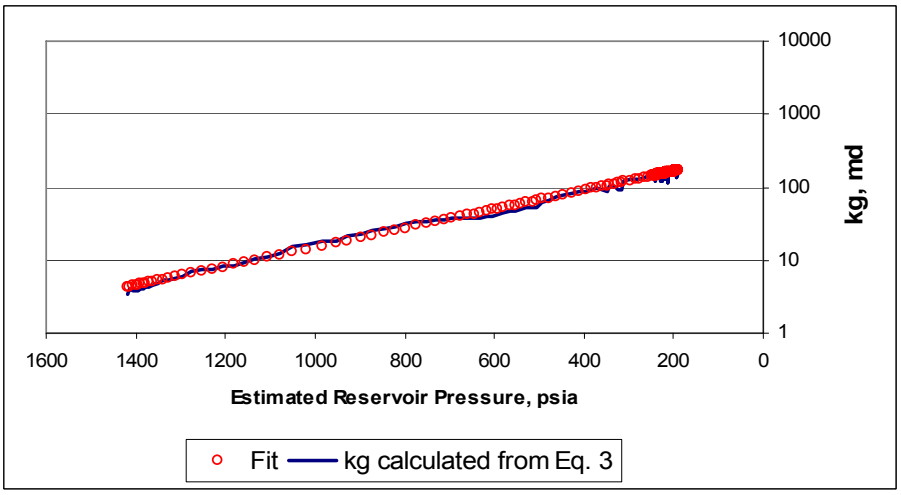

(b)

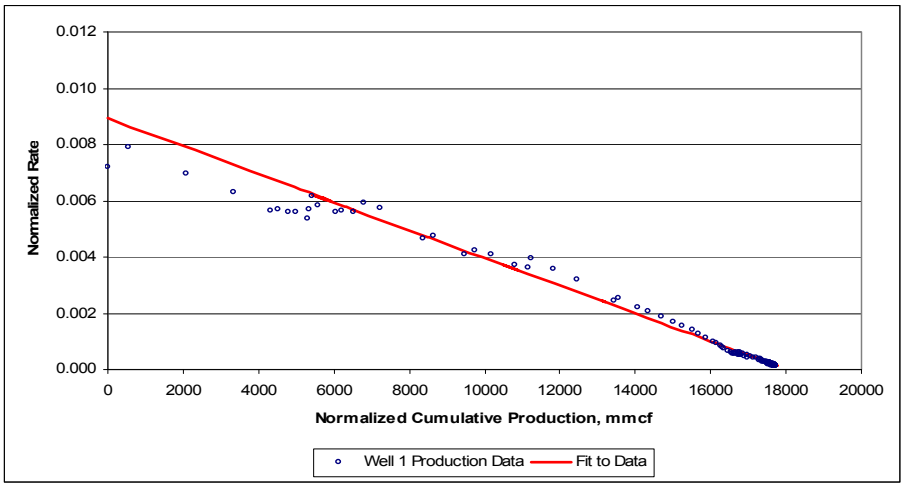

(c)

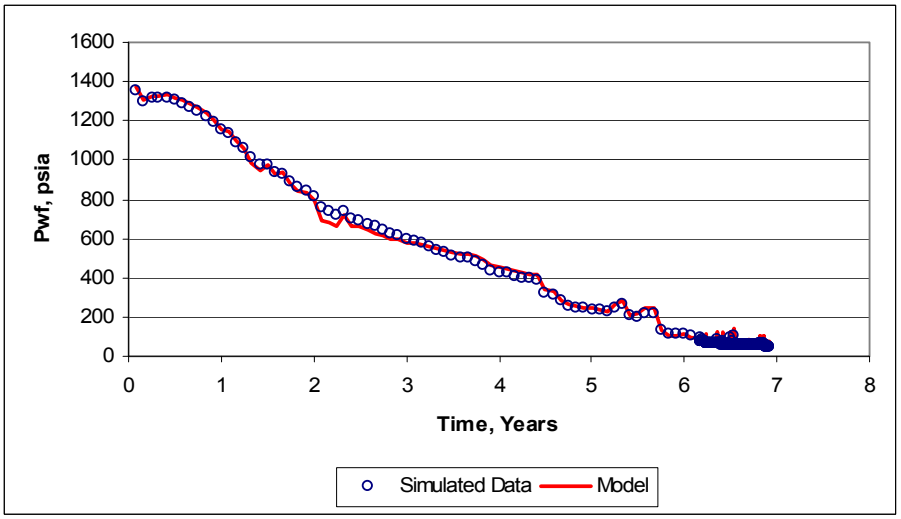

Fig. 13 — Well 1 modeling results : (a) match to k_g calculated with Eq. 3; (b) FMB plot and; (c) analytical model match to flowing bottomhole pressure (numerical simulator match to actual data).

(a)

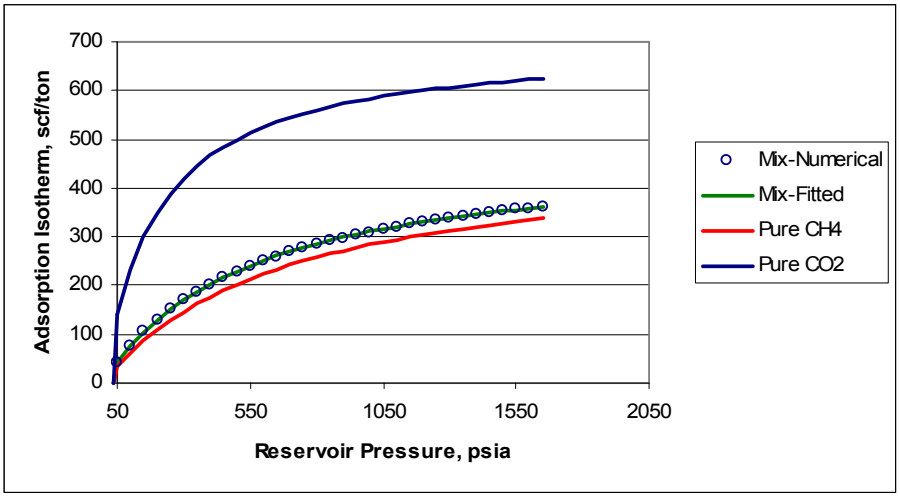

(b)

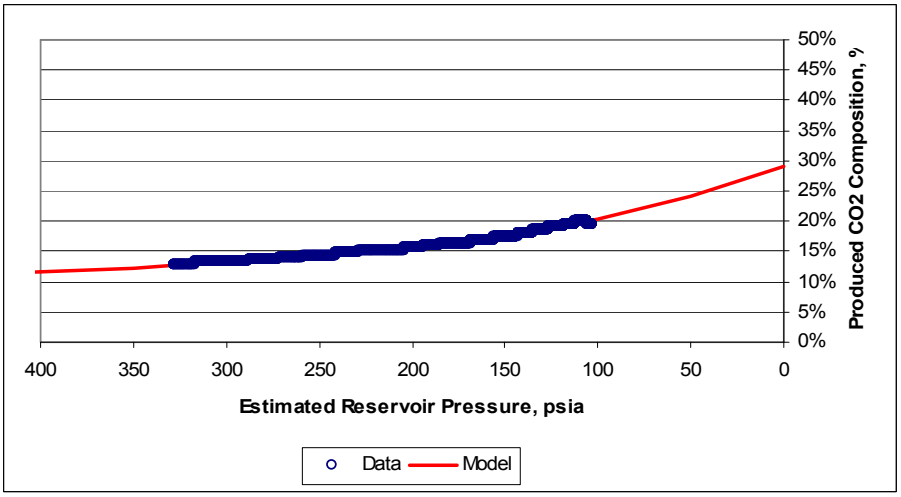

(c)

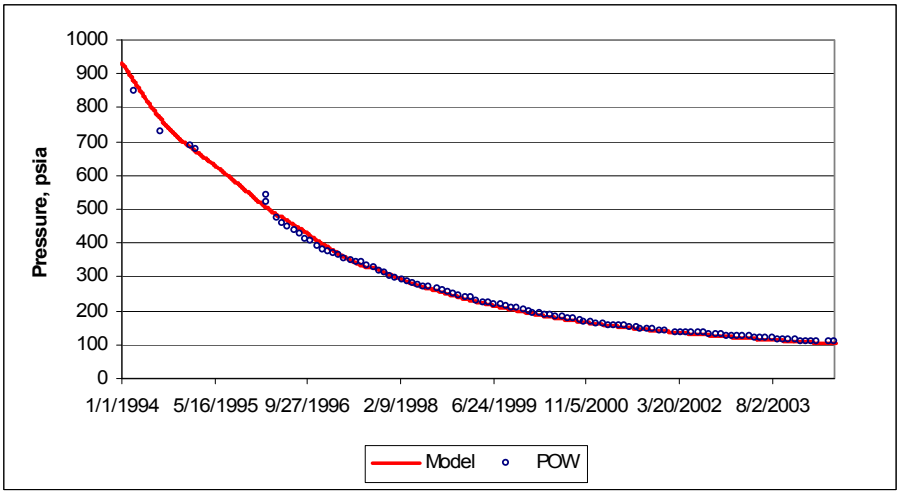

Fig. 14 — Well 2 modeling results : (a) individual and composite isotherms used to match produced gas compositions; ; (b) match of gas compositions with HP technique; (c) match to offset pressure observation well (POW) data.

(a)

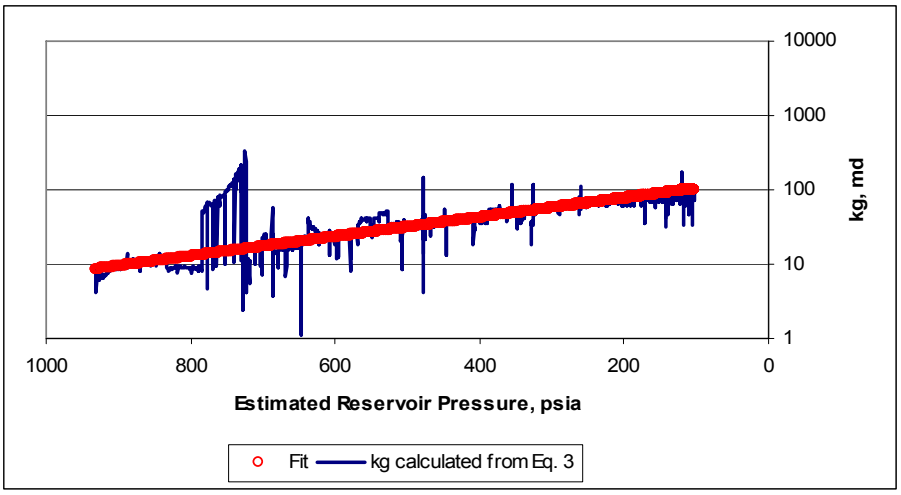

(b)

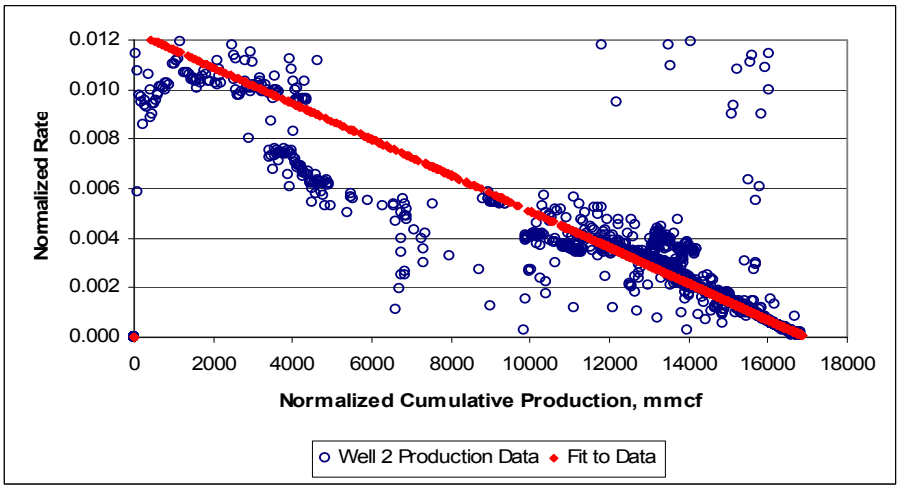

(c)

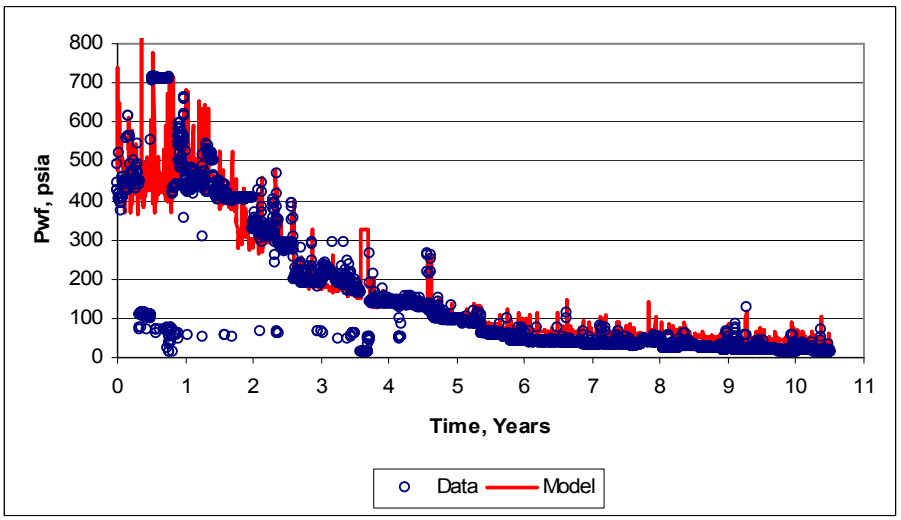

Fig. 15 — Well 2 modeling results : (a) match to k_g calculated with Eq. 3; (b) FMB plot and; (c) analytical model match to flowing bottomhole pressure.